iScience

CellPress
OPEN ACCESS

Article

Interaction of RSC Chromatin Remodeling Complex with Nucleosomes Is Modulated by H3 K14 Acetylation and H2B SUMOylation *In Vivo*

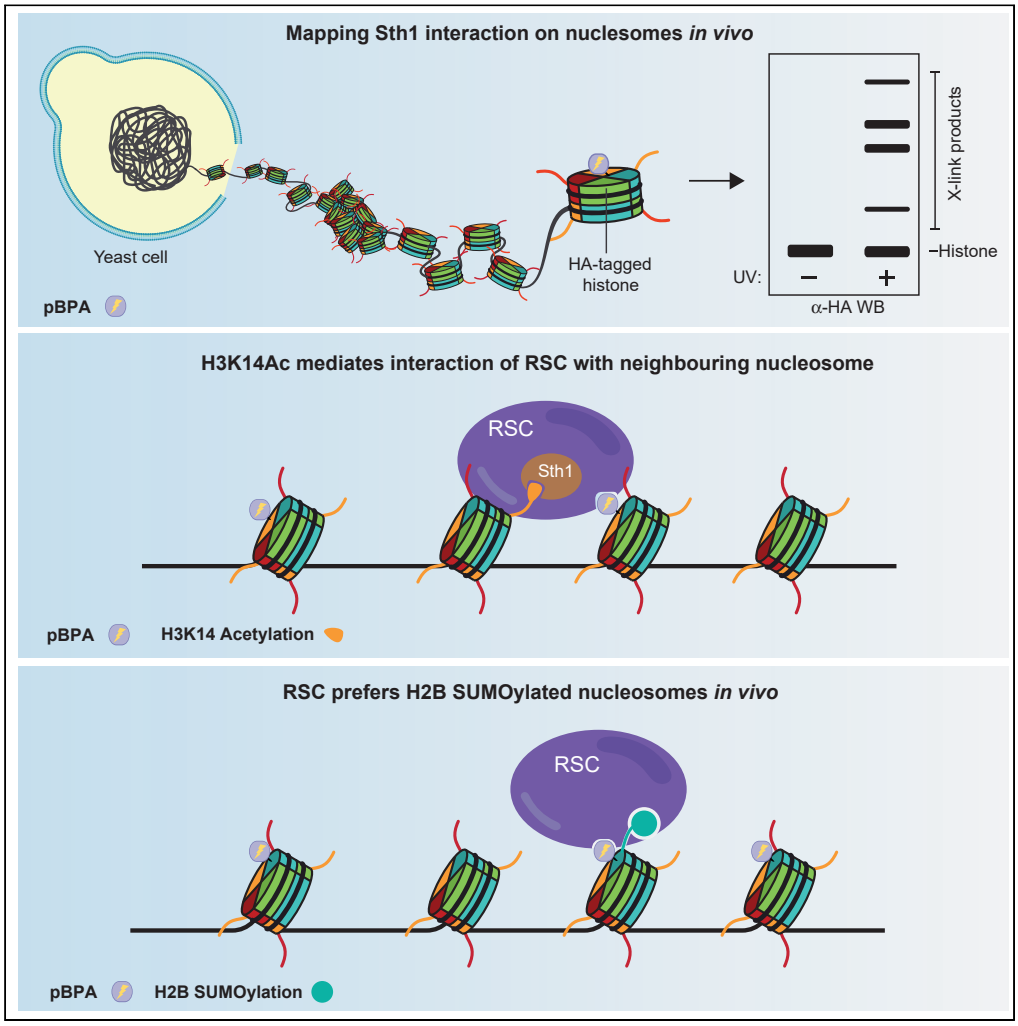

Neha Jain, Davide Tamborrini, Brian Evans, Shereen Chaudhry, Bryan J. Wilkins, Heinz Neumann

bwilkins01@manhattan.edu (B.J.W.)
heinz.neumann@mpi-dortmund.mpg.de (H.N.)

HIGHLIGHTS

Footprint of ATPase subunit of RSC on the nucleosome by *in vivo* photo-cross-linking

C-terminal bromodomain of ATPase-subunit Sth1 binds H3 K14ac

RSC preferentially localizes to H2B-SUMOylated nucleosomes

Jain et al., iScience *23*, 101292
July 24, 2020 © 2020 The Authors.
https://doi.org/10.1016/j.isci.2020.101292

iScience

CellPress
OPEN ACCESS

Article

Interaction of RSC Chromatin Remodeling Complex with Nucleosomes Is Modulated by H3 K14 Acetylation and H2B SUMOylation *In Vivo*

Neha Jain,[1,4] Davide Tamborrini,[1,4] Brian Evans,[2] Shereen Chaudhry,[2] Bryan J. Wilkins,[2,*] and Heinz Neumann[1,3,5,*]

SUMMARY

Chromatin remodeling complexes are multi-subunit nucleosome translocases that reorganize chromatin in the context of DNA replication, repair, and transcription. To understand how these complexes find their target sites on chromatin, we use genetically encoded photo-cross-linker amino acids to map the footprint of Sth1, the catalytic subunit of the RSC complex, on nucleosomes in living yeast. We find that H3 K14 acetylation induces the interaction of the Sth1 bromodomain with the H3 tail and mediates the interaction of RSC with neighboring nucleosomes rather than recruiting it to chromatin. RSC preferentially resides on H2B SUMOylated nucleosomes *in vivo* and shows a moderately enhanced affinity due to this modification *in vitro*. Furthermore, RSC is not ejected from chromatin in mitosis, but changes its mode of nucleosome binding. Our *in vivo* analyses show that RSC recruitment to specific chromatin targets involves multiple histone modifications likely in combination with histone variants and transcription factors.

INTRODUCTION

Storage and accessibility of genetic information are two conflicting requirements that a cell must balance. While the DNA must be compacted to meet the space limitations of the nucleus, access to its information content for transcription, repair, and replication processes must be ensured. Eukaryotes accomplish this by packaging their DNA in chromatin; however, densely packed chromatin territories restrict the accessibility of the underlying DNA (Padeken and Heun, 2014). Hence, to facilitate access to DNA, chromatin has evolved highly malleable properties to meet the demands for dynamic changes (Seeber and Gasser, 2017; Talbert and Henikoff, 2017; Tessarz and Kouzarides, 2014).

Chromatin remodeling enzymes use ATP hydrolysis to rearrange nucleosomes to enable other factors to access DNA (Clapier et al., 2017). Posttranslational modifications (PTMs) of histones and histone variants either modulate the stability and DNA-binding properties of the nucleosome or signal the recruitment of machinery that initiates the transcription, replication, or repair of DNA (Tessarz and Kouzarides, 2014). The turnover of most histone PTMs is rapid, making these processes very dynamic.

Common to all families of chromatin remodelers are an affinity for nucleosomes, the ability to recognize histone PTMs via specialized domains, and a DNA-dependent ATPase domain that translocates DNA relative to the histone octamer. Apart from that, remodelers differ significantly in subunit composition, specificity for histone modifications, the processes in which they are involved, and whether they promote chromatin opening or closing. How these enzymes work, how their activity is regulated, and how they are recruited to specific loci are currently being actively investigated.

The RSC complex is an abundant, essential chromatin remodeling complex of the SWI/SNF family in budding yeast (Cairns et al., 1996). RSC is involved in transcription (Brahma and Henikoff, 2018; Floer et al., 2010; Krietenstein et al., 2016; Musladin et al., 2014; Spain et al., 2014), chromosome segregation (Hsu et al., 2003), replication (Niimi et al., 2012), and the response to DNA damage (Rowe and Narlikar, 2010; Shim et al., 2007).

Recently, the high-resolution structure of the RSC complex bound to a nucleosome has been solved by cryo-electron microscopy, revealing three flexibly connected domains (Patel et al., 2019; Wagner et al.,

[1]Department of Structural Biochemistry, Max-Planck-Institute of Molecular Physiology, Otto-Hahn-Strasse 11, 44227 Dortmund, Germany

[2]Department of Chemistry and Biochemistry, Manhattan College, 4513 Manhattan College Parkway, Bronx, NY 10471, USA

[3]Department of Chemical Engineering and Biotechnology, University of Applied Sciences Darmstadt, Stephanstrasse 7, 64295 Darmstadt, Germany

[4]These authors contributed equally

[5]Lead Contact

*Correspondence: bwilkins01@manhattan.edu (B.J.W.), heinz.neumann@mpi-dortmund.mpg.de (H.N.)

https://doi.org/10.1016/j.isci.2020.101292

This is an open access article under the CC BY-NC-ND license (http://creativecommons.org/licenses/by-nc-nd/4.0/).

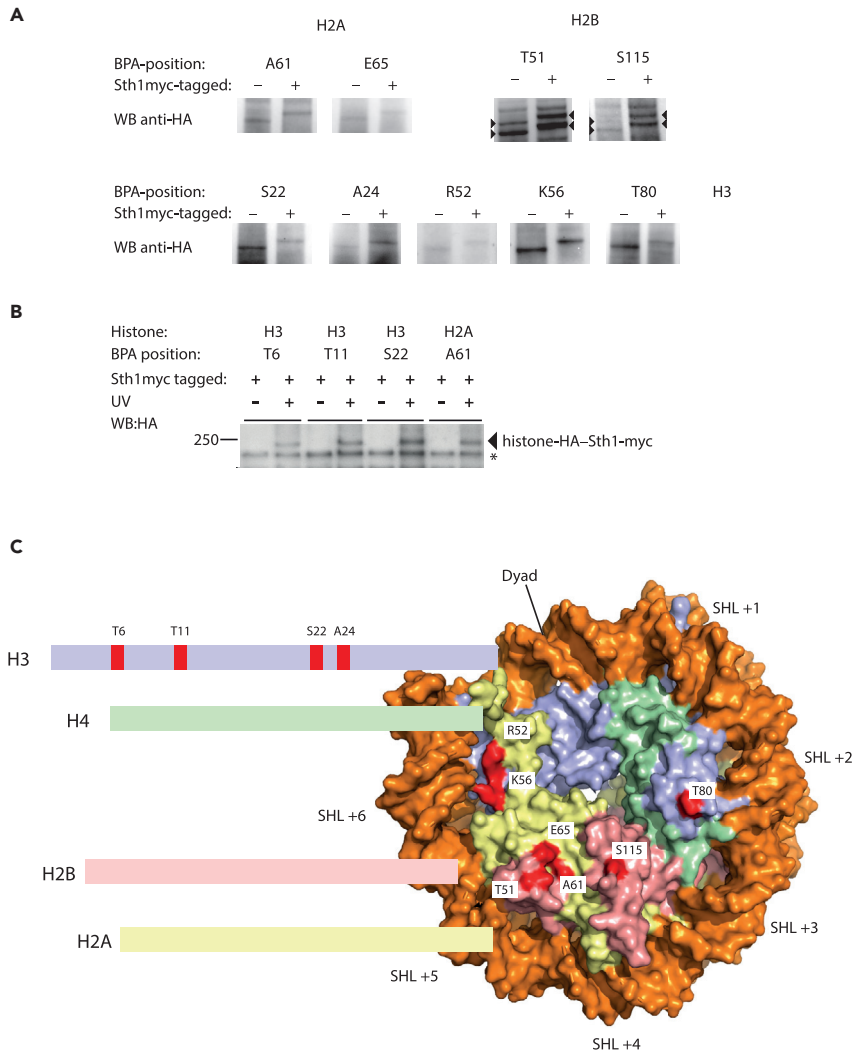

Figure 1. Mapping the Interaction Surface of Sth1 on the Nucleosome *In Vivo*

(A) Yeast cells (wild-type or Sth1-3myc) expressing histones with pBPA at the indicated position were UV irradiated and cross-link products analyzed by SDS-PAGE and western blot using anti-HA antibodies recognizing the pBPA-containing histone. The shift in mobility resulting from the myc-tag identifies a cross-link product with Sth1. H2B-Sth1 cross-links appear as a double band due to H2B SUMOylation (arrow heads). See Figures S1–S6 for full-sized western blots.

(B) Cross-link reactions from positions in the H3 tail performed in Sth1-3myc cells were subjected to immunoprecipitation with anti-myc antibody beads prior to analysis by western blot with anti-HA antibodies. The Sth1-histone cross-link is indicated by the arrowhead. A cross-reactive band is marked by an asterisk.

(C) Graphical representation of the positions identified in (A) and (B) on the structure of the nucleosome. Figure was prepared using PDB: 1ID3 and PyMol v1.7.6.6.

2020; Ye et al., 2019). The motor domain of the Sth1 subunit binds at superhelical location (SHL) +2, from where it translocates the DNA one base pair at a time into the direction of the dyad, possibly creating a loop that propagates around the nucleosome (Zhang et al., 2006). The ARP module, which couples DNA translocation and ATPase activity (Clapier et al., 2016), connects the motor domain to the substrate recognition module (SRM). The latter contains DNA-binding Zn-cluster domains, five bromodomains, a histone-tail-binding BAH domain, and the nucleosome-binding C-terminal tail of Sfh1 (Patel et al., 2019; Wagner et al., 2020; Ye et al., 2019). Owing to the flexible tethering of these domains, their structure, substrate preference, and interaction with the nucleosome remained largely unresolved. The only established lysine acetylation site on histones recognized by RSC is H3 K14ac by the bromodomains of Sth1 and Rsc4 (Chen et al., 2020; Kasten et al., 2004; VanDemark et al., 2007).

Here, we use quantitative *in vivo* cross-linking with genetically encoded photo-activatable cross-linker amino acids to reveal the footprint of the Sth1 subunit of RSC on the nucleosome. The interaction of Sth1 with the N-terminal H3 tail depends on the presence of H3 K14, which is recognized by the C-terminal bromodomain of Sth1 upon acetylation (Chen et al., 2020). We further show that Sth1 preferentially cross-links to the SUMOylated form of H2B, suggesting that H2B SUMOylation acts in the context of RSC remodeling.

RESULTS

In Vivo Cross-linking Survey of the Nucleosome

Genetic code expansion allows for the incorporation of unnatural amino acids (UAAs) in response to amber (UAG) stop codons in a variety of cells and organisms (Neumann-Staubitz and Neumann, 2016). In yeast, this is achieved by transforming the cells with a plasmid encoding an evolved aminoacyl-tRNA synthetase specific for the desired UAA and its cognate amber suppressor tRNA. A second plasmid is introduced encoding the gene of interest with an amber codon replacing the codon for the amino acid that shall be converted to the UAA. In these cells, the evolved aminoacyl-tRNA synthetase charges its cognate tRNA with the UAA, which is subsequently incorporated at the site specified by the amber codon in the protein of interest.

We have established the incorporation of photo-activatable cross-linker amino acids in histones and chromatin-interacting proteins to study the dynamics of chromatin in living yeast (Hoffmann and Neumann, 2015; Wilkins et al., 2014). The cross-linking reaction follows a long-wavelength UV light (365 nm)-inducible radical mechanism that results in the formation of binary covalent adducts that can be quantitated by western blot (Dorman and Prestwich, 1994).

To map the interactome of the nucleosome in living yeast, we created a library of more than one hundred amber mutants covering the surface-exposed residues of the nucleosome. We incorporated *p*-benzoyl-L-phenylalanine (pBPA) in response to amber stop codons by genetic code expansion for each individual mutant and analyzed cross-link products formed upon irradiation by SDS-PAGE and western blot against the HA-epitope on the histone (Figures S1 and S2).

Cross-link scans of the nucleosomal surface revealed differential binding patterns across each of the histones, highlighting the viability of interactome mapping in the living nucleus. We then asked if this approach could be employed to characterize individual chromatin binding proteins, specifically nucleosome bound chromatin remodeling complexes.

Footprint of Sth1, the Catalytic Subunit of RSC, on the Nucleosome

In order to probe the footprint of the catalytic subunit of RSC, Sth1, on the nucleosome surface we selected 58 histone pBPA mutants from the cross-linking survey that had produced a band of appropriate combined mass for a cross-link product of a histone with Sth1 (approximately 170 kDa). To test whether these bands indeed result from cross-linking to Sth1 we performed the same cross-linking reaction in strains with or without a C-terminal 3xmyc-tag on Sth1 (Figure 1 and S3–S6). The epitope tag leads to a slower migration of the corresponding band of the cross-link product in western blots. This analysis identified nine positions on the nucleosome core and H3 tail that interact with Sth1 (Figure 1A). We detected two further positions in the H3 tail (T6 and T11), when we precipitated the cross-link products with anti-myc antibody beads (against myc-tagged Sth1) prior to western blot analysis with anti-HA antibodies (Figure 1B). This confirmed the ability of pBPA at these positions to cross-link to Sth1.

When we measured the growth rates of cells expressing the pBPA-containing histones, we observed a moderate reduction, indicating that the amber suppressor system, the fragment produced by termination at the amber stop codon, or the mutated histones stress the cells to some extent (Figure S7). However, we expect that the biological role of RSC and its interaction with the nucleosome is comparable with the native state because the mutant histone represents only a small fraction of the total amount. To visualize the footprint of Sth1 on the nucleosome, we mapped these positions on the structure of the nucleosome core particle (Figure 1C).

Binding of the H3 Tail by Sth1 Depends on H3 K14

We hypothesized that the C-terminal bromodomain of Sth1 might mediate the interaction with the H3 tail because H3 K14 acetylation enhances nucleosome binding by RSC (Duan and Smerdon, 2014) and a recent

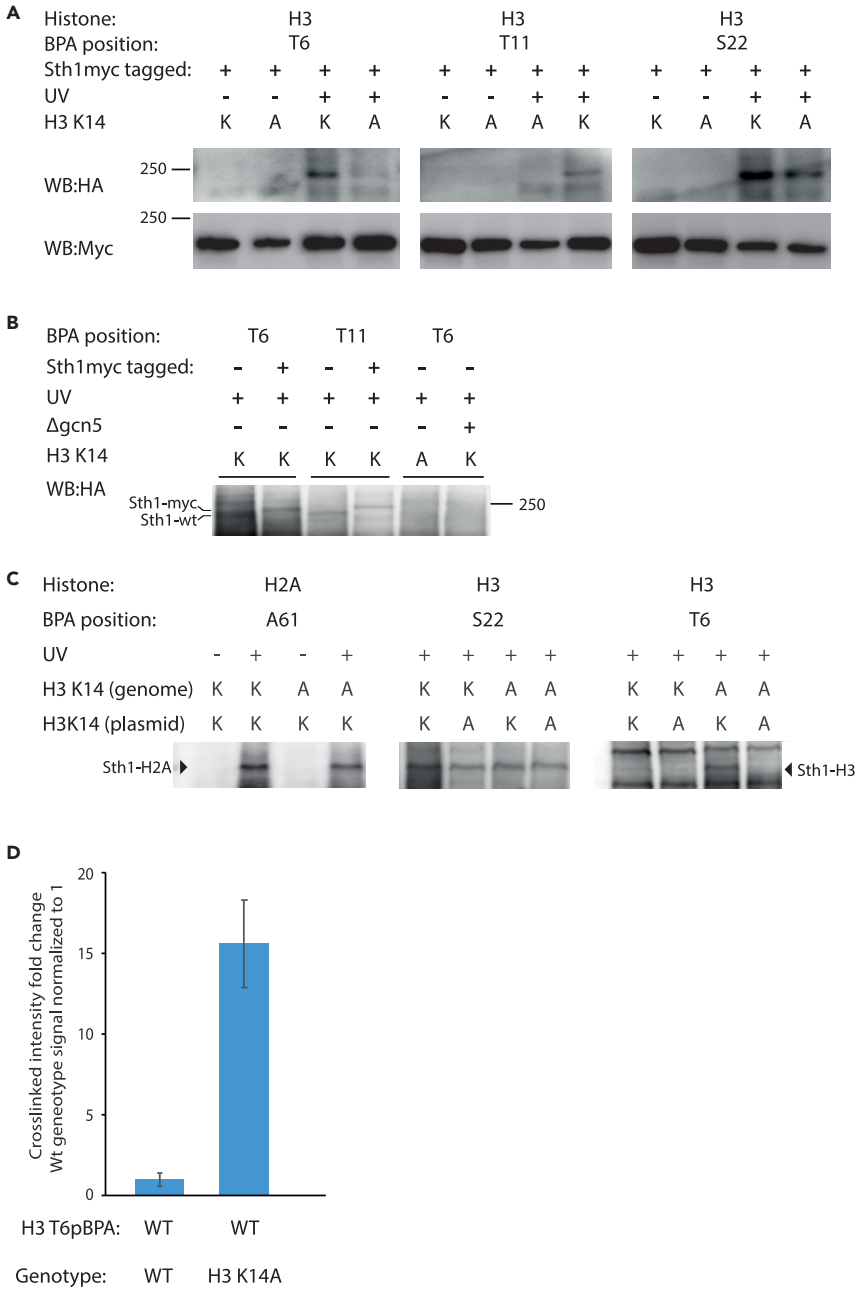

Figure 2. Cross-linking of the H3 Tail to Sth1 Is Regulated by H3 K14ac

(A) Cross-linking from positions in the H3 tail in Sth1-3myc cells. Anti-myc immunoprecipitates were analyzed by western blot with anti-HA antibodies.

(B) Deletion of *gcn5* interferes with H3 T6pBPA cross-linking to Sth1. WCEs of cross-linked samples were irradiated with UV light and whole-cell extracts analyzed by western blot using anti-HA antibodies.

(C) Effect of mutating endogenous H3 K14 to alanine on cross-linking to Sth1. Yeasts (wild-type or H3 K14A) expressing H3 T6pBPA, H3 S22pBPA, or H2A A61pBPA with or without K14A mutation were analyzed as in (B).

(D) Quantitative comparison of cross-linking efficiencies from H3 T6pBPA in wild-type and H3 K14A yeasts. Error bars are standard deviations of five independent experiments.

co-crystal structure revealed an extensive interface between the Sth1 bromodomain and an H3 tail peptide (Chen et al., 2020). We therefore mutated H3 K14 to alanine on the same H3 copy containing pBPA. The mutation interfered with cross-linking of H3 T6pBPA and T11pBPA to Sth1, whereas cross-linking from

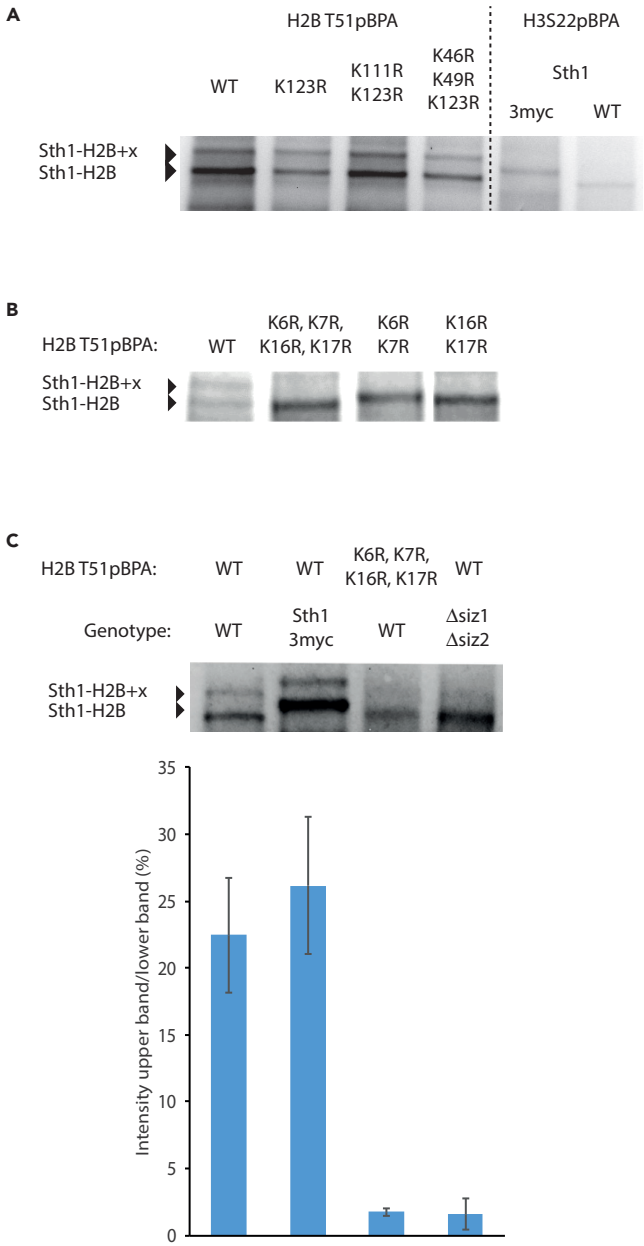

Figure 3. RSC Prefers Binding of H2B SUMOylated Nucleosomes

(A) Cross-link pattern of H2B T51pBPA is not affected by mutation in lysine residues reported to be subject to ubiquitinylation. Cross-links to H3 S22pBPA are used as reference to identify Sth1-H2B cross-link.

(B) Effect of mutating H2B SUMOylation sites on H2B T51pBPA cross-link pattern.

(C) Effect of deletion of *siz1* and *siz2* on H2B T51pBPA cross-link pattern. Intensities of upper and lower cross-link bands were quantified by densitometry. Error bars are standard deviations of five independent experiments. In all panels, yeasts expressing H2B T51pBPA with the indicated mutations were UV-irradiated and whole-cell lysates analyzed by SDS-PAGE and western blot using anti-HA antibodies. Full blots in Figure S8.

H3 S22pBPA was only partially affected by K14A, suggesting that K14 is required for the interaction of Sth1 with the tip of the H3 tail (Figure 2A).

In order to demonstrate that acetylation of H3 K14 is essential for this interaction, we deleted the gene encoding lysine acetyltransferase Gcn5, the enzyme responsible for the deposition of H3 K14ac (Kuo et al.,

1996; Zhang et al., 1998). This indeed abolished cross-linking between the H3 tail and Sth1, much like the H3 K14A mutation (Figure 2B).

Next, we asked whether H3 K14ac serves to recruit RSC to nucleosomes. Therefore, we performed cross-linking experiments from H2A A61pBPA-nucleosomes in yeast with or without a genomic H3 K14A mutation (Figure 2C, left panel) (Dai et al., 2008). We observed that cross-linking of Sth1 was only slightly reduced by the K14A mutation. Hence, recruitment of RSC to chromatin does not require H3 K14ac, otherwise the cross-linking efficiency from this position would have been reduced in the mutant background.

This is consistent with the micromolar concentration of nucleosomes in the yeast nucleus (approximately 60,000 nucleosomes [Oberbeckmann et al., 2019] in a volume of 3 fL [Jorgensen et al., 2007]) being more than one thousand times greater than the dissociation constant (K_D) of RSC-nucleosome complexes (Lorch et al., 1998). Therefore, increasing the affinity of RSC for nucleosomes by histone modifications is not expected to enhance the level of saturation (Θ) of RSC with nucleosomes because Θ is hardly affected by changes in ligand concentration if their concentration is greater than ten times K_D.

However, H3 K14ac may control which nucleosomes are bound by RSC. In this case, mutation of H3 K14 in nucleosomes without the cross-linker (i.e., in the genomic copy of the H3 gene) should shift RSC binding to cross-linker-containing nucleosomes that still possess H3 K14ac.

Therefore, we performed cross-linking experiments from H3 S22 in the background of a yeast strain bearing the K14A mutation in the genomic copy of H3 (Figure 2C, middle panel). If H3 K14ac recruits RSC to nucleosomes, this mutation should increase the cross-linking efficiency because the cross-linker-containing nucleosomes are the only ones with an intact H3 K14 residue. However, cross-linking from H3 S22pBPA was not affected by genomic H3 K14A mutation; hence, H3 K14ac does not control recruitment of RSC.

Finally, we asked whether the Sth1 bromodomain exclusively interacts with H3 tails that are part of the nucleosome bound by RSC or whether H3 tails from neighboring nucleosomes are also substrates. Therefore, we performed cross-linking experiments from H3 T6pBPA in the genetic background of H3 K14A cells (Figure 2C, right panel). If the bromodomain of Sth1 only interacts with H3 tails that are part of the same nucleosome that the complex is bound to, the mutation of the endogenous H3 should not affect the cross-linking efficiency. However, if Sth1 interacts with H3 tails of neighboring nucleosomes, the mutation would abrogate the competition with their histone tails and therefore increase cross-linking. Indeed, the K14A mutation of the endogenous H3 allele increased cross-linking between Sth1 and H3 T6pBPA 15-fold (Figure 2D), strongly indicating that the bromodomain of Sth1 is able to interact with acetylated H3 tails of other nucleosomes.

RSC Preferentially Interacts with SUMOylated H2B *In Vivo*

Cross-link products of Sth1 to histones H2A and H3 each migrated as a single band in western blots with an apparent molecular mass of about 180 kDa (Figure 1). H2B-Sth1 cross-link products (from positions T51 and S115), however, showed a second band shifted by approximately 10 kDa to a higher apparent mass (Figure 1). Initially, we hypothesized that this mass shift is a result of H2B K123 ubiquitination, the major site of H2B ubiquitination in budding yeast (Robzyk et al., 2000). However, the cross-linking pattern of ubiquitination-deficient mutant H2B T51pBPA K123R was indistinguishable from that of H2B T51pBPA (Figure 3A). Hence, we tested additional H2B sites known to be ubiquitinated (K46, K49, and K111) (Swaney et al., 2013), which also did not change the cross-linking pattern (Figure 3A). Next, we analyzed the impact of mutating combinations of K6, K7, K16, and K17 in H2B T51pBPA to arginine on cross-linking to Sth1 (Figure 3B). These are the major sites of H2B SUMOylation in *S. cerevisiae* (Nathan et al., 2006). Indeed, in the absence of these lysine residues, we observed only a single H2B-Sth1 cross-link product. Interestingly, mutating either pair of lysine residues in the H2B N terminus (K6/7 or K16/17) was sufficient to abolish the slower migrating band. Accordingly, mutations of the same sites have previously been shown to abolish H2B SUMOylation (Nathan et al., 2006). Finally, when we analyzed a strain lacking E3 SUMO ligases Siz1 and Siz2 required for H2B SUMOylation (Nathan et al., 2006), the cross-link reaction produced only a single H2B-Sth1 band (Figure 3C), unambiguously confirming the upper band to be the SUMOylated form of H2B.

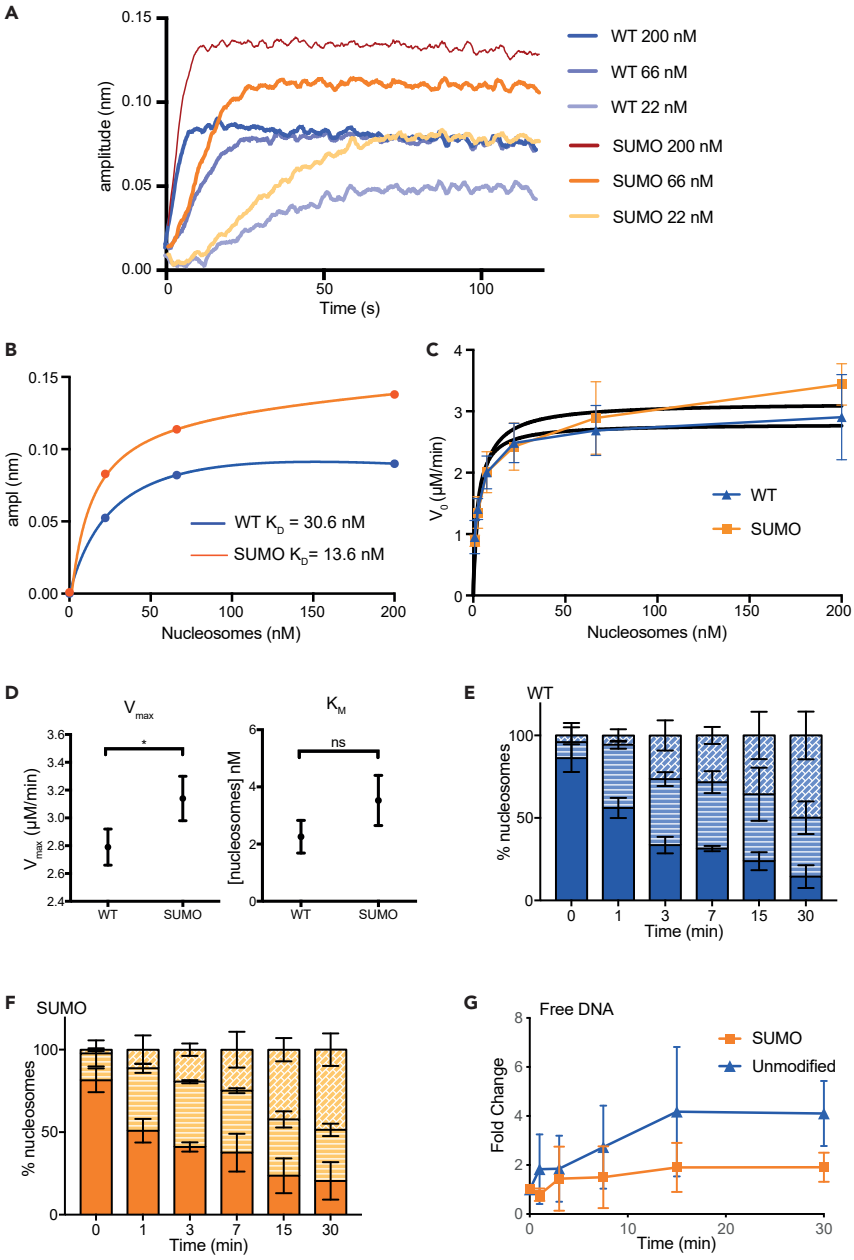

Figure 4. *In Vitro* Characterization of RSC-nucleosome Affinity and Activity

(A) Biotinylated RSC complex was immobilized on streptavidin biolayer tips and nucleosome (167-bp Widom-601 DNA) binding was analyzed by BLI at different concentrations of nucleosomes (0, 22, 66, 200 nM). See Figure S11 for raw data file.

(B) K_D values were determined by fitting the amplitudes of each binding kinetic with GraphPad.

(C) V_0 values of RSC remodeling reactions (determined with an ADP-Glo Assay) at different concentrations of unmodified and SUMOylated nucleosomes (0.8, 2.5, 7.5, 22, 66, 200 nM; 197bp Widom-601 DNA) fit to a Michaelis-Menten equation.

(D) V_{max} and K_M determined from data shown in (C) for unmodified (2.79 $\pm$ 0.13 μM/min; 2.25 $\pm$ 0.56 nM) and SUMOylated nucleosomes (3.14 $\pm$ 0.16 μM/min; 3.52 $\pm$ 0.87 nM).

(E) RSC nucleosome remodeling activity (in the presence of Nap1) by EMSA. The relative amounts of unremodeled (top part of the bar) and two remodeled species (middle and bottom) were quantified for unmodified (WT) (197bp Widom-601 DNA).

(F) Same as E but for SUMOylated nucleosomes.

(G) The amount of ejected DNA in EMSA was determined densitometrically and normalized to the initial amount of free DNA. All error bars are standard deviations of the means of at least three independent experiments. A typical EMSA gel is shown in Figure S12.

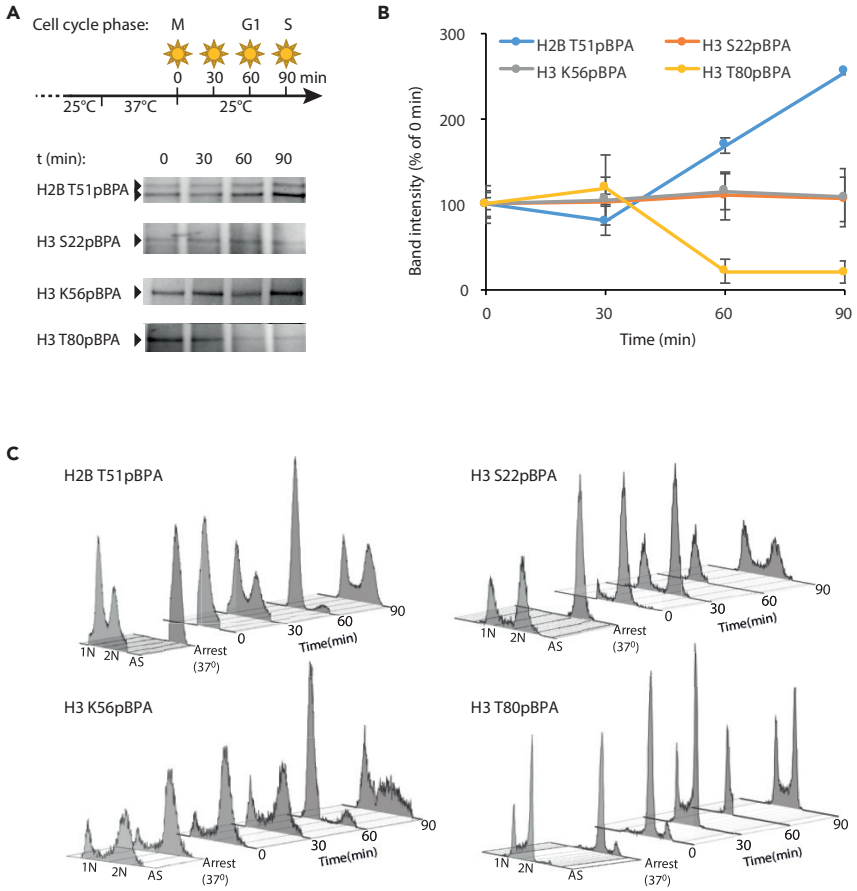

Figure 5. Effect of the Cell Cycle Stage on Histone-Sth1 Cross-link Efficiency

(A) Yeasts (*cdc15-2*) expressing the indicated pBPA-containing histones were synchronized using the illustrated temperature-shift protocol. Samples were irradiated and whole-cell lysates analyzed by SDS-PAGE and western blot using anti-HA antibodies.

(B) Band intensities of three to four independent replicates of the experiment shown in (A) were quantified by densitometry using Fuji software (see Transparent Methods for details). Error bars are standard errors of the mean. Full blots in Figure S13.

(C) Fluorescence-activated cell sorting (FACS) analysis of synchronized yeast populations analyzed in (A) and (B).

Densitometric quantification of both bands indicates that 20%–30% of H2B that interacts with Sth1 is SUMOylated.

Impact of H2B SUMOylation on RSC *In Vitro*

In order to reveal the impact of H2B SUMOylation on the interaction of RSC with nucleosomes, we produced nucleosomes containing an in-frame fusion of SUMO to H2B (*Xenopus* sequence truncated by the first five N-terminal residues, Figure S9). RSC complex purified from yeast (see Transparent Methods and Figure S10) bound to SUMOylated nucleosomes with approximately 2-fold higher affinity than to unmodified nucleosomes in the presence of the non-hydrolysable ATP analog AMP-PNP in biolayer interferometry (BLI) experiments (Figures 4A, 4B, and S11). To further analyze RSC action on nucleosomes, we compared the rate of ATP hydrolysis by RSC in the presence of SUMOylated and unmodified nucleosomes (Figures 4C and 4D). We observed a slightly increased activity on SUMOylated nucleosomes without a change in catalytic efficiency ($V_{max}/c(RSC)/K_M$). Similarly, the rate of nucleosome remodeling by RSC in electromobility shift assays was not affected by H2B SUMOylation (Figures 4E and 4F). However, we observed a reduced amount of free DNA in remodeling reactions with SUMOylated nucleosomes, suggesting that the modification may have an influence on the ejection of the octamer during remodeling (Figure 4G). Altogether our data suggest that SUMOylation of H2B per se only has a modest role in RSC

affinity and activity *in vitro* and most likely synergizes with other factors in the recruitment of RSC to chromatin *in vivo*.

Modulation of Sth1-Nucleosome Interactions during the Cell Cycle

Chromatin compaction in mitosis is thought to counteract transcription by preventing access of transcription factors, RNA polymerase, and chromatin remodelers to DNA (Yokoyama and Gruss, 2013). To test whether RSC binding to chromatin is influenced by chromatin structure, we analyzed the cross-linking efficiency of histones to Sth1 during the cell cycle (Figure 5). Therefore, we synchronized temperature-sensitive *cdc15-2* yeasts harboring plasmids to produce the pBPA-containing histones using a temperature shift protocol. We then sampled over time, cross-linked, and analyzed the cross-link products by SDS-PAGE and western blot. Of the four positions studied, two (H3 S22 and K56) displayed a constant cross-linking efficiency between mitosis and interphase, indicating that the RSC remodeling complex remains bound to nucleosomes throughout the cell cycle. For the other two positions (H3 T80 and H2B T51), however, we observed a reciprocal change in intensity between mitosis and interphase, indicating that chromatin structure has a subtle influence on how RSC binds nucleosomes.

DISCUSSION

We analyzed more than one hundred sites in core histones for their suitability for pBPA incorporation and cross-linking. Many sites gave rise to abundant and diverse cross-link products. Identification of the cross-link partners is the limiting step to proteome-wide mapping of chromatin interacting proteins. Ideally, this could be done by mass spectrometry, which has been established for mammalian cells (Kleiner et al., 2018) and should also be feasible in yeast. However, because of the large number of different cross-link products formed from the same position on histone proteins, the amount of material of each individual cross-link product is very low. This restricts quantitative measurements by mass spectrometry, which are essential for the investigation of the impact of mutations or the cell cycle on the interactions.

Here, we explored whether cross-link products to Sth1 were present in the cross-linking patterns using electrophoretic mobility shift assays (EMSAs) to reveal the footprint of the protein on the nucleosome *in vivo*. Drawing on structural information of the nucleosome-bound RSC complex (Wagner et al., 2020; Ye et al., 2019), cross-link reactions from the H3 αN-helix (R52, K56) most likely target the motor domain of Sth1, consistent with the observation that mutations in this helix have a strong effect on RSC remodeling activity (Somers and Owen-Hughes, 2009).

Positions on the nucleosome surface (H2A A61, E65; H2B T51, S115; H3 T80) most likely cross-link to the SnaC domain of Sth1 (Wagner et al., 2020), whereas positions in the H3-tail probably target its bromodomain in agreement with recent structural studies (Chen et al., 2020). The RSC complex therefore contacts the acidic patches on both sides of the nucleosome simultaneously, with Sth1 SnaC on one side and with Sfh1 (Wagner et al., 2020) on the other.

Our observations further show that H3 K14 acetylation is required for the interaction of the H3 tail with Sth1. Binding of the RSC complex to nucleosomes, however, is little affected by removing this mark indicating that its recruitment is controlled by additional mechanisms, e.g., general regulatory factors of transcription and DNA sequence motifs (Krietenstein et al., 2016). Our data suggest that the bromodomain of Sth1 binds the K14ac mark of H3 tails of neighboring nucleosomes. This property would be well compatible with the idea that RSC contributes to the formation of a nucleosome-free region at yeast promoters (Krietenstein et al., 2016; Wippo et al., 2011).

Interestingly, position H3 T80 and H2B T51 show reciprocal changes in cross-linking intensities between mitosis and interphase (Figure 5). We speculate that the RSC-nucleosome interaction is modulated by changes in chromatin structure during the cell cycle. Since the cross-linking efficiencies from two other sites (H3 S22 and K56) displayed hardly any changes at different cell cycle stages, we conclude that RSC activity is not controlled by eviction of the remodeler from chromatin by condensation in mitosis, as has been observed for the homologous human chromatin remodeler BRG-1 (Muchardt et al., 1996).

Alternatively, the changes in cross-linking efficiencies with the cell cycle stages might be the result of cell cycle variations in histone PTMs. For example, H3 K56ac displays pronounced cell cycle variation (Ozdemir et al., 2006). Although H3 K56ac does not affect RSC binding and remodeling, it may affect RSC binding at

the αN-helix of H3 (Neumann et al., 2009). Incorporation of pBPA at this position ablates acetylation and would be consistent with a loss of cell cycle-dependent cross-linking.

Our cross-linking experiments revealed a previously unreported preference of RSC for H2B SUMOylated nucleosomes. The cross-linking reactions from H2B positions produced a double band with the upper band being about 20%–30% of the lower band intensity. In contrast, SUMOylation affects only about 5% of H2B molecules (Nathan et al., 2006), implying that RSC has a strong thermodynamic preference for these nucleosomes. However, our biochemical analyses do not support this conclusion. Alternatively, RSC may be trapped kinetically at such sites by mediating the deposition of the modification through recruitment of the SUMOylation machinery. Indeed, RSC subunits were identified in a Siz1 pull-down (Srikumar et al., 2013). Future experiments should address whether H2B SUMOylation modulates RSC activity *in vivo* or whether H2B SUMOylation depends on RSC activity.

Limitations of the Study

Our approach may be useful to study the preference of protein complexes for particular histone variants. For example, it has been shown that RSC preferentially remodels H2A.Z-containing nucleosomes at promoters (Cakiroglu et al., 2019). By comparing cross-linking efficiencies from equivalent positions between two histone variants, it should be possible to identify such preferences. Specifically, cross-linking from positions close to the acidic patch of canonical H2A and H2A.Z could be used to test whether RSC preferentially resides on nucleosomes with the latter variant. However, in order to allow such comparisons, expression levels of both isoforms must be carefully balanced.

Resource Availability

Lead Contact

Further information and requests for resources and reagents should be directed to and will be fulfilled by the Lead Contact, Heinz Neumann (heinz.neumann@mpi-dortmund.mpg.de or heinz.neumann@h-da.de).

Materials Availability

All unique/stable reagents generated in this study are available from the Lead Contact with a completed Materials Transfer Agreement, if there is potential for commercial application.

Data and Code Availability

This study did not generate datasets or code.

METHODS

All methods can be found in the accompanying Transparent Methods supplemental file.

SUPPLEMENTAL INFORMATION

Supplemental Information can be found online at https://doi.org/10.1016/j.isci.2020.101292.

ACKNOWLEDGMENTS

We thank Petra Geue, Simon Herrmann, and Corinna Krüger for technical assistance; Roger Goody for help with analyzing kinetic data; and Andrea Musacchio for sharing reagents and his comments on the manuscript. We thank Daniela Rhodes, Fabrizio Martino, and Dirk Görlich for providing plasmids.

This project was supported by the German Research Foundation (DFG) (Grants NE1589/5-1 and 6-1), the Human Frontier Science Program (HFSP, RPG0031/2017), and the Max-Planck-Institute of Molecular Physiology to H.N. Both B.J.W. and B.E. were supported by the National Institute of General Medical Sciences of the National Institutes of Health under Award Number R15GM124600. The content is solely the responsibility of the authors and does not necessarily represent the official views of the National Institutes of Health. B.J.W. and S.C. received support from the Michael Kakos and Aimee Rusinko Kakos Faculty Fellowship.

AUTHOR CONTRIBUTIONS

Conceptualization, B.J.W. and H.N.; Methodology, N.J., D.T., B.W.J.; Investigation, N.J., D.T., B.E., S.C., B.J.W., H.N.; Writing – Original Draft, N.J., D.T., B.J.W., H.N.; Writing – Review & Editing, N.J., D.T.,

B.J.W., H.N.; Supervision, B.J.W., H.N.; Project Administration, B.J.W., H.N.; Funding Acquisition, B.J.W., H.N.

DECLARATION OF INTERESTS

The authors declare that no competing interests exist.

Received: May 12, 2020
Revised: May 27, 2020
Accepted: June 15, 2020
Published: July 24, 2020

REFERENCES

Brahma, S., and Henikoff, S. (2018). RSC-associated subnucleosomes define MNase-sensitive promoters in yeast. Mol. Cell *73*, 238–249.

Cairns, B.R., Lorch, Y., Li, Y., Zhang, M., Lacomis, L., Erdjument-Bromage, H., Tempst, P., Du, J., Laurent, B., and Kornberg, R.D. (1996). RSC, an essential, abundant chromatin-remodeling complex. Cell *87*, 1249–1260.

Cakiroglu, A., Clapier, C.R., Ehrensberger, A.H., Darbo, E., Cairns, B.R., Luscombe, N.M., and Svejstrup, J.Q. (2019). Genome-wide reconstitution of chromatin transactions reveals that RSC preferentially disrupts H2AZ-containing nucleosomes. Genome Res. *29*, 988–998.

Chen, G.C., Li, W., Yan, F.X., Wang, D., and Chen, Y. (2020). The structural basis for specific recognition of H3K14 acetylation by Sth1 in the RSC chromatin remodeling complex. Structure *28*, 111–118.e3.

Clapier, C.R., Iwasa, J., Cairns, B.R., and Peterson, C.L. (2017). Mechanisms of action and regulation of ATP-dependent chromatin-remodelling complexes. Nat. Rev. Mol. Cell Biol. *18*, 407–422.

Clapier, C.R., Kasten, M.M., Parnell, T.J., Viswanathan, R., Szerlong, H., Sirinakis, G., Zhang, Y.L., and Cairns, B.R. (2016). Regulation of DNA translocation efficiency within the chromatin remodeler RSC/Sth1 potentiates nucleosome sliding and ejection. Mol. Cell *62*, 453–461.

Dai, J., Hyland, E.M., Yuan, D.S., Huang, H., Bader, J.S., and Boeke, J.D. (2008). Probing nucleosome function: a highly versatile library of synthetic histone H3 and H4 mutants. Cell *134*, 1066–1078.

Dorman, G., and Prestwich, G.D. (1994). Benzophenone photophores in biochemistry. Biochemistry *33*, 5661–5673.

Duan, M.R., and Smerdon, M.J. (2014). Histone H3 lysine 14 (H3K14) acetylation facilitates DNA repair in a positioned nucleosome by stabilizing the binding of the chromatin Remodeler RSC (Remodels Structure of Chromatin). J. Biol. Chem. *289*, 8353–8363.

Floer, M., Wang, X., Prabhu, V., Berrozpe, G., Narayan, S., Spagna, D., Alvarez, D., Kendall, J., Krasnitz, A., Stepansky, A., et al. (2010). A RSC/nucleosome complex determines chromatin architecture and facilitates activator binding. Cell *141*, 407–418.

Hoffmann, C., and Neumann, H. (2015). In vivo mapping of FACT-histone interactions identifies a role of Pob3 C-terminus in H2A-H2B binding. ACS Chem. Biol. *10*, 2753–2763.

Hsu, J.M., Huang, J., Meluh, P.B., and Laurent, B.C. (2003). The yeast RSC chromatin-remodeling complex is required for kinetochore function in chromosome segregation. Mol. Cell. Biol. *23*, 3202–3215.

Jorgensen, P., Edgington, N.P., Schneider, B.L., Rupes, I., Tyers, M., and Futcher, B. (2007). The size of the nucleus increases as yeast cells grow. Mol. Biol. Cell *18*, 3523–3532.

Kasten, M., Szerlong, H., Erdjument-Bromage, H., Tempst, P., Werner, M., and Cairns, B.R. (2004). Tandem bromodomains in the chromatin remodeler RSC recognize acetylated histone H3 Lys14. EMBO J. *23*, 1348–1359.

Kleiner, R.E., Hang, L.E., Molloy, K.R., Chait, B.T., and Kapoor, T.M. (2018). A chemical proteomics approach to reveal direct protein-protein interactions in living cells. Cell Chem. Biol. *25*, 110–120.e3.

Krietenstein, N., Wal, M., Watanabe, S., Park, B., Peterson, C.L., Pugh, B.F., and Korber, P. (2016). Genomic nucleosome organization reconstituted with pure proteins. Cell *167*, 709–721 e712.

Kuo, M.H., Brownell, J.E., Sobel, R.E., Ranalli, T.A., Cook, R.G., Edmondson, D.G., Roth, S.Y., and Allis, C.D. (1996). Transcription-linked acetylation by Gcn5p of histones H3 and H4 at specific lysines. Nature *383*, 269–272.

Lorch, Y., Cairns, B.R., Zhang, M.C., and Kornberg, R.D. (1998). Activated RSC-nucleosome complex and persistently altered form of the nucleosome. Cell *94*, 29–34.

Muchardt, C., Reyes, J.C., Bourachot, B., Leguoy, E., and Yaniv, M. (1996). The hbrm and BRG-1 proteins, components of the human SNF/SWI complex, are phosphorylated and excluded from the condensed chromosomes during mitosis. EMBO J. *15*, 3394–3402.

Musladin, S., Krietenstein, N., Korber, P., and Barbaric, S. (2014). The RSC chromatin remodeling complex has a crucial role in the complete remodeler set for yeast PHO5 promoter opening. Nucleic Acids Res. *42*, 4270–4282.

Nathan, D., Ingvarsdottir, K., Sterner, D.E., Bylebyl, G.R., Dokmanovic, M., Dorsey, J.A., Whelan, K.A., Krsmanovic, M., Lane, W.S., Meluh, P.B., et al. (2006). Histone sumoylation is a negative regulator in *Saccharomyces cerevisiae* and shows dynamic interplay with positive-acting histone modifications. Genes Dev. *20*, 966–976.

Neumann, H., Hancock, S.M., Buning, R., Routh, A., Chapman, L., Somers, J., Owen-Hughes, T., van Noort, J., Rhodes, D., and Chin, J.W. (2009). A method for genetically installing site-specific acetylation in recombinant histones defines the effects of H3 K56 acetylation. Mol. Cell *36*, 153–163.

Neumann-Staubitz, P., and Neumann, H. (2016). The use of unnatural amino acids to study and engineer protein function. Curr. Opin. Struct. Biol. *38*, 119–128.

Niimi, A., Chambers, A.L., Downs, J.A., and Lehmann, A.R. (2012). A role for chromatin remodellers in replication of damaged DNA. Nucleic Acids Res. *40*, 7393–7403.

Oberbeckmann, E., Wolff, M., Krietenstein, N., Heron, M., Ellins, J.L., Schmid, A., Krebs, S., Blum, H., Gerland, U., and Korber, P. (2019). Absolute nucleosome occupancy map for the *Saccharomyces cerevisiae* genome. Genome Res. *29*, 1996–2009.

Ozdemir, A., Masumoto, H., Fitzjohn, P., Verreault, A., and Logie, C. (2006). Histone H3 lysine 56 acetylation: a new twist in the chromosome cycle. Cell Cycle *5*, 2602–2608.

Padeken, J., and Heun, P. (2014). Nucleolus and nuclear periphery: velcro for heterochromatin. Curr. Opin. Cell Biol. *28*, 54–60.

Patel, A.B., Moore, C.M., Greber, B.J., Luo, J., Zukin, S.A., Ranish, J., and Nogales, E. (2019). Architecture of the chromatin remodeler RSC and insights into its nucleosome engagement. Elife *8*, e54449.

Robzyk, K., Recht, J., and Osley, M.A. (2000). Rad6-dependent ubiquitination of histone H2B in yeast. Science *287*, 501–504.

Rowe, C.E., and Narlikar, G.J. (2010). The ATP-dependent remodeler RSC transfers histone dimers and octamers through the rapid formation of an unstable encounter intermediate. Biochemistry *49*, 9882–9890.

Seeber, A., and Gasser, S.M. (2017). Chromatin organization and dynamics in double-strand break repair. Curr. Opin. Genet. Dev. *43*, 9–16.

Shim, E.Y., Hong, S.J., Oum, J.H., Yanez, Y., Zhang, Y., and Lee, S.E. (2007). RSC mobilizes nucleosomes to improve accessibility of repair machinery to the damaged chromatin. Mol. Cell Biol. *27*, 1602–1613.

Somers, J., and Owen-Hughes, T. (2009). Mutations to the histone H3 alpha N region selectively alter the outcome of ATP-dependent nucleosome-remodelling reactions. Nucleic Acids Res. *37*, 2504–2513.

Spain, M.M., Ansari, S.A., Pathak, R., Palumbo, M.J., Morse, R.H., and Govind, C.K. (2014). The RSC complex localizes to coding sequences to regulate Pol II and histone occupancy. Mol. Cell *56*, 653–666.

Srikumar, T., Lewicki, M.C., and Raught, B. (2013). A global S. cerevisiae small ubiquitin-related modifier (SUMO) system interactome. Mol. Syst. Biol. *9*, 668.

Swaney, D.L., Beltrao, P., Starita, L., Guo, A., Rush, J., Fields, S., Krogan, N.J., and Villen, J. (2013). Global analysis of phosphorylation and ubiquitylation cross-talk in protein degradation. Nat. Methods *10*, 676–682.

Talbert, P.B., and Henikoff, S. (2017). Histone variants on the move: substrates for chromatin dynamics. Nat. Rev. Mol. Cell Biol. *18*, 115–126.

Tessarz, P., and Kouzarides, T. (2014). Histone core modifications regulating nucleosome structure and dynamics. Nat. Rev. Mol. Cell Biol. *15*, 703–708.

VanDemark, A.P., Kasten, M.M., Ferris, E., Heroux, A., Hill, C.P., and Cairns, B.R. (2007). Autoregulation of the rsc4 tandem bromodomain by gcn5 acetylation. Mol. Cell *27*, 817–828.

Wagner, F.R., Dienemann, C., Wang, H., Stützer, A., Tegunov, D., Urlaub, H., and Cramer, P. (2020). Structure of SWI/SNF chromatin remodeller RSC bound to a nucleosome. Nature *579*, 448–451.

Wilkins, B.J., Rall, N.A., Ostwal, Y., Kruitwagen, T., Hiragami-Hamada, K., Winkler, M., Barral, Y., Fischle, W., and Neumann, H. (2014). A cascade of histone modifications induces chromatin condensation in mitosis. Science *343*, 77–80.

Wippo, C.J., Israel, L., Watanabe, S., Hochheimer, A., Peterson, C.L., and Korber, P. (2011). The RSC chromatin remodelling enzyme has a unique role in directing the accurate positioning of nucleosomes. EMBO J. *30*, 1277–1288.

Ye, Y., Wu, H., Chen, K., Clapier, C.R., Verma, N., Zhang, W., Deng, H., Cairns, B.R., Gao, N., and Chen, Z. (2019). Structure of the RSC complex bound to the nucleosome. Science *366*, 838–843.

Yokoyama, H., and Gruss, O.J. (2013). New mitotic regulators released from chromatin. Front Oncol. *3*, 308.

Zhang, W., Bone, J.R., Edmondson, D.G., Turner, B.M., and Roth, S.Y. (1998). Essential and redundant functions of histone acetylation revealed by mutation of target lysines and loss of the Gcn5p acetyltransferase. EMBO J. *17*, 3155–3167.

Zhang, Y., Smith, C.L., Saha, A., Grill, S.W., Mihardja, S., Smith, S.B., Cairns, B.R., Peterson, C.L., and Bustamante, C. (2006). DNA translocation and loop formation mechanism of chromatin remodeling by SWI/SNF and RSC. Mol. Cell *24*, 559–568.

iScience, Volume *23*

Supplemental Information

Interaction of RSC Chromatin Remodeling Complex with Nucleosomes Is Modulated by H3 K14 Acetylation and H2B SUMOylation *In Vivo*

Neha Jain, Davide Tamborrini, Brian Evans, Shereen Chaudhry, Bryan J. Wilkins, and Heinz Neumann

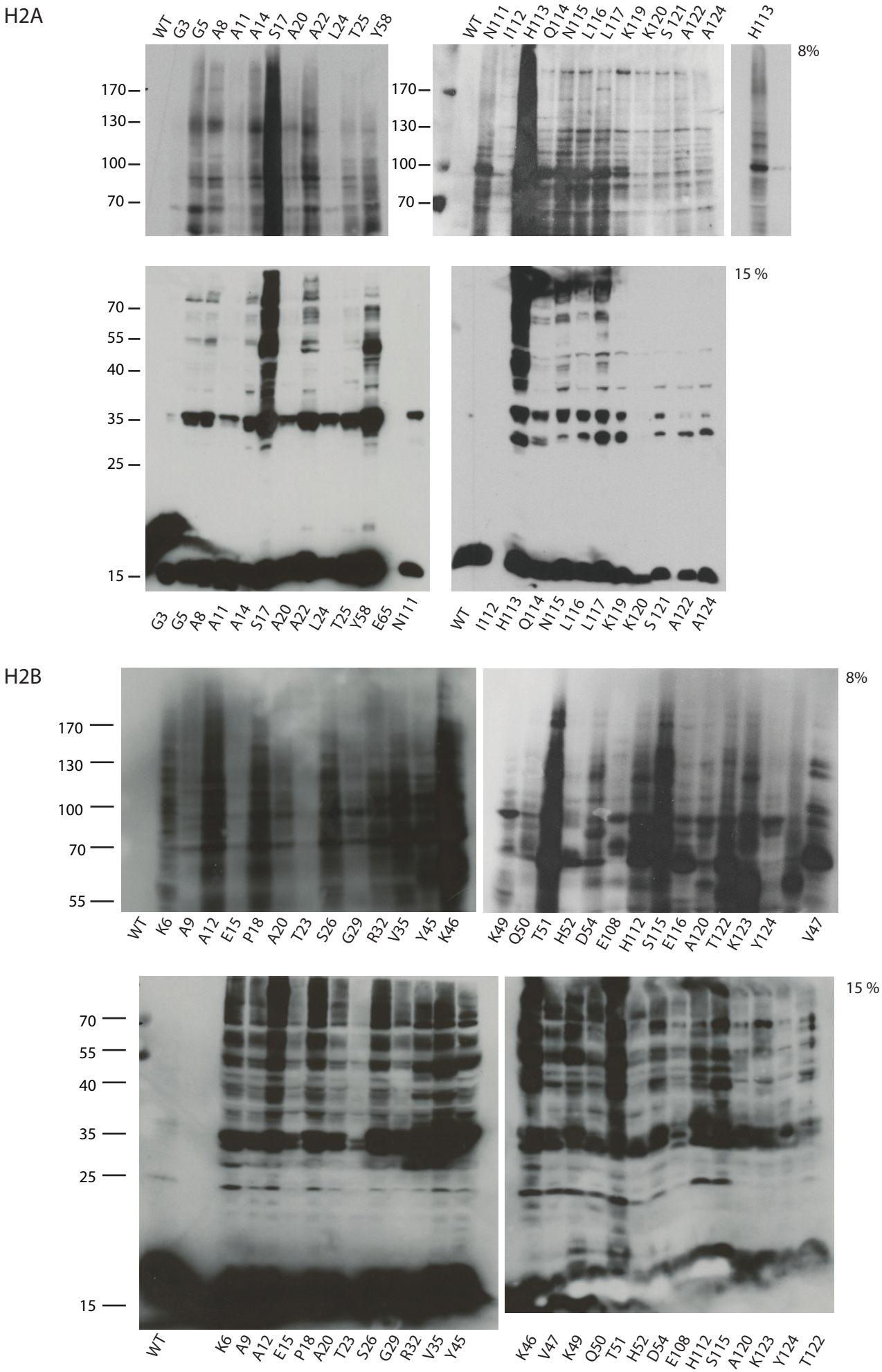

Supplemental Figure 1: Western Blot analyses of histone H2A- and H2B-pBPA crosslink products. Full-sized Western blot to Figure 1. Yeasts expressing the indicated pBPA-containing histone were UV-irradiated and whole cell lysates analysed by SDS-PAGE and Western Blot using anti-HA antibodies.

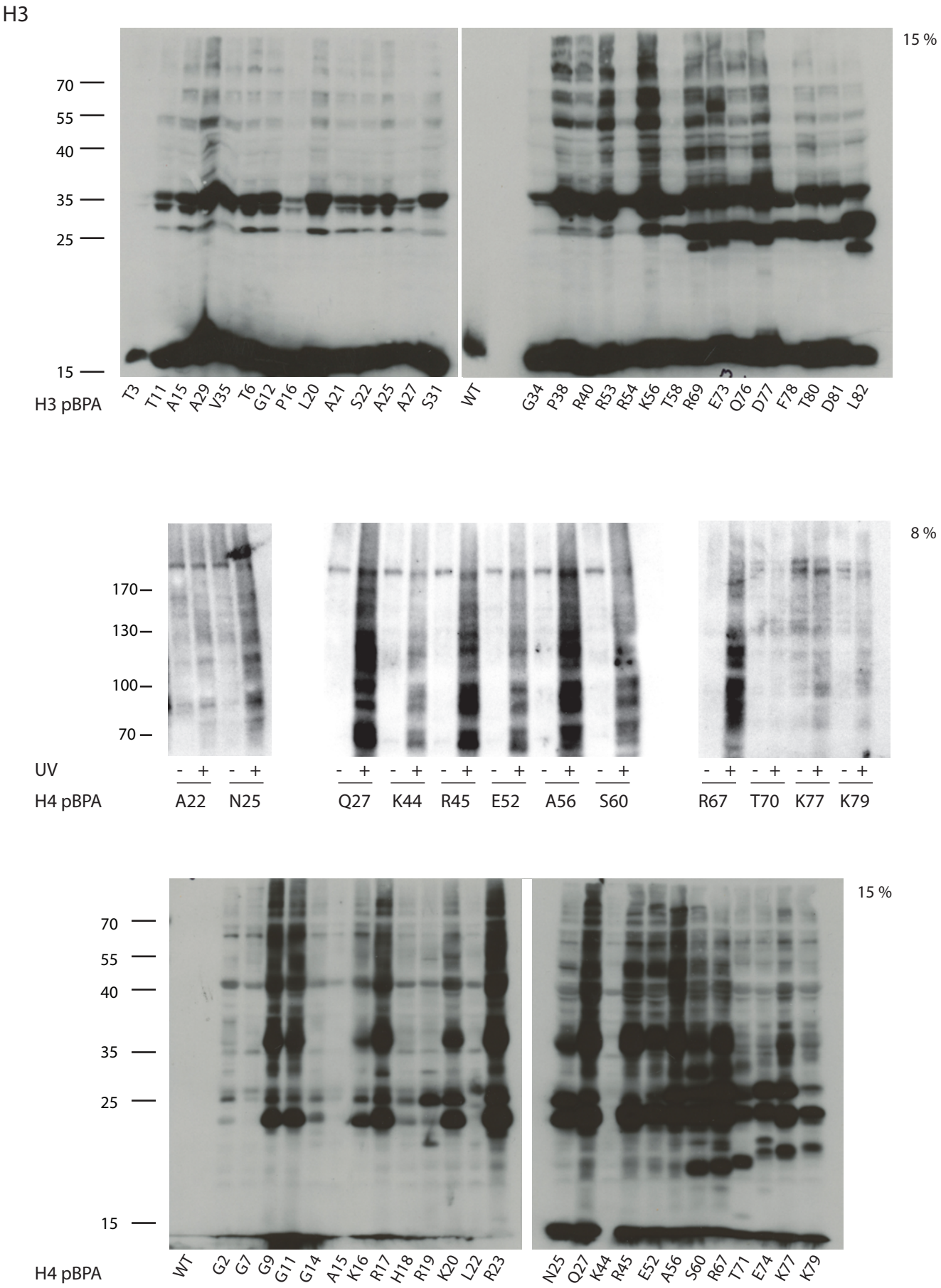

Supplemental Figure 2: Western Blot analyses of histone H3- and H4-pBPA crosslink products. Full-sized Western blot to Figure 1. Yeasts expressing the indicated pBPA-containing histone were UV-irradiated and whole cell lysates analysed by SDS-PAGE and Western Blot using anti-HA antibodies.

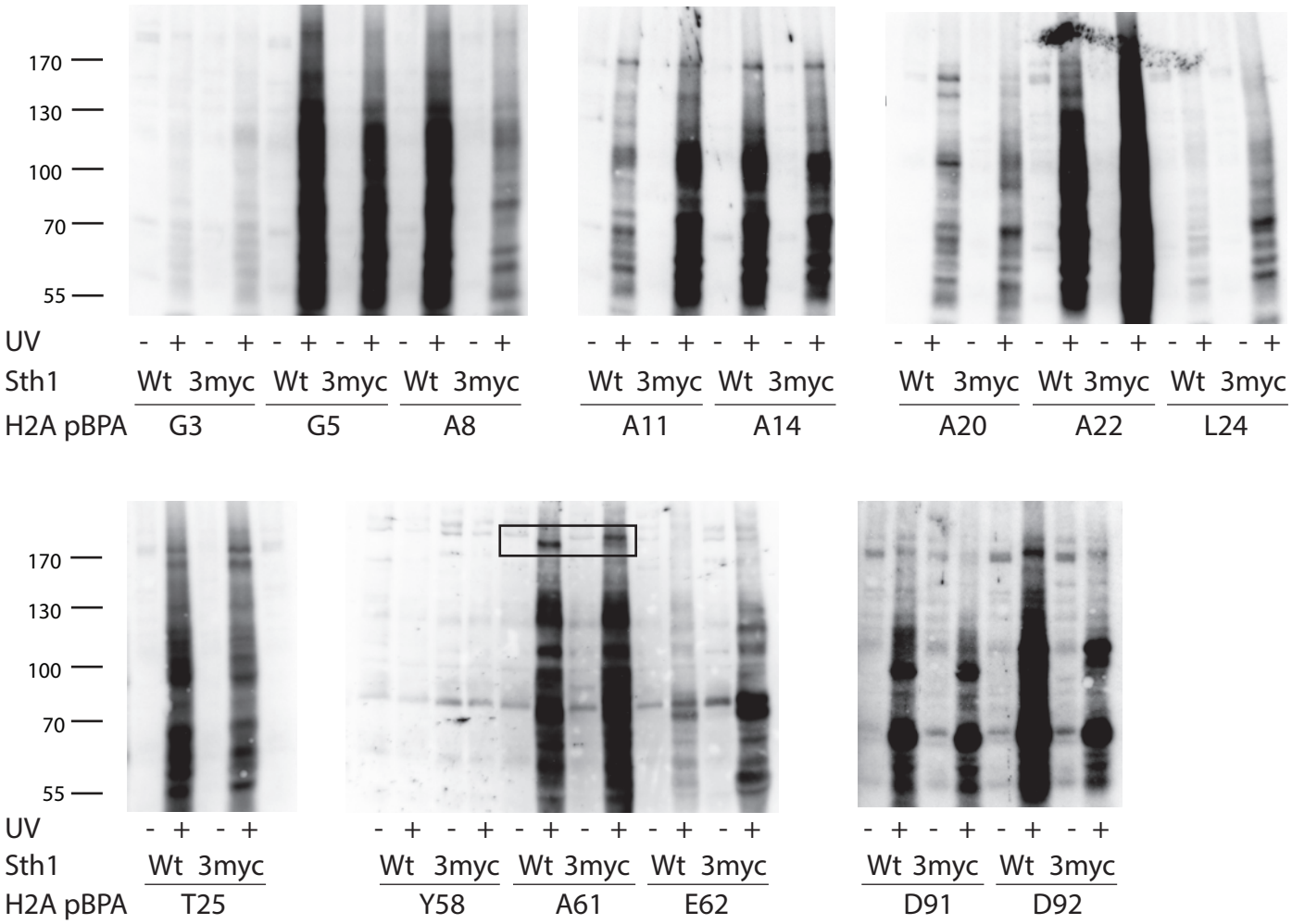

Supplemental Figure 3: Identification of Sth1-histone H2A crosslink products. Full-sized Western blots to Figure 1. Yeasts (wild-type or Sth1-3myc) expressing the indicated pBPA-containing histone were UV-irradiated and whole cell lysates analysed by SDS-PAGE and Western Blot using anti-HA antibodies. Boxed areas show bands sensitive to Sth1-tagging.

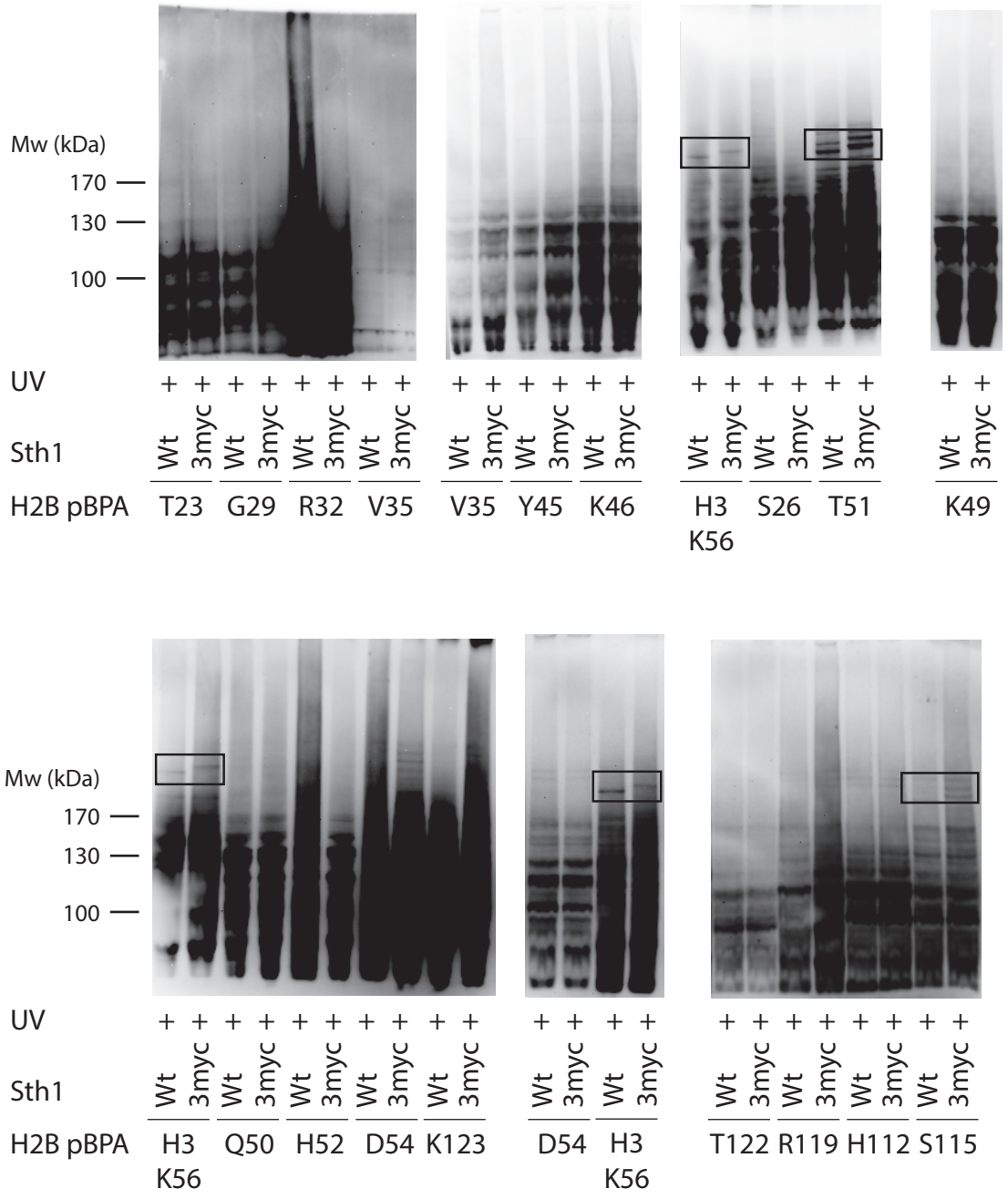

Supplemental Figure 4: Identification of Sth1-histone H2B crosslink products. Full-sized Western blots to Figure 1. Yeasts (wild-type or Sth1-3myc) expressing the indicated pBPA-containing histone were UV-irradiated and whole cell lysates analysed by SDS-PAGE and Western Blot using anti-HA antibodies. Boxed areas show bands sensitive to Sth1-tagging.

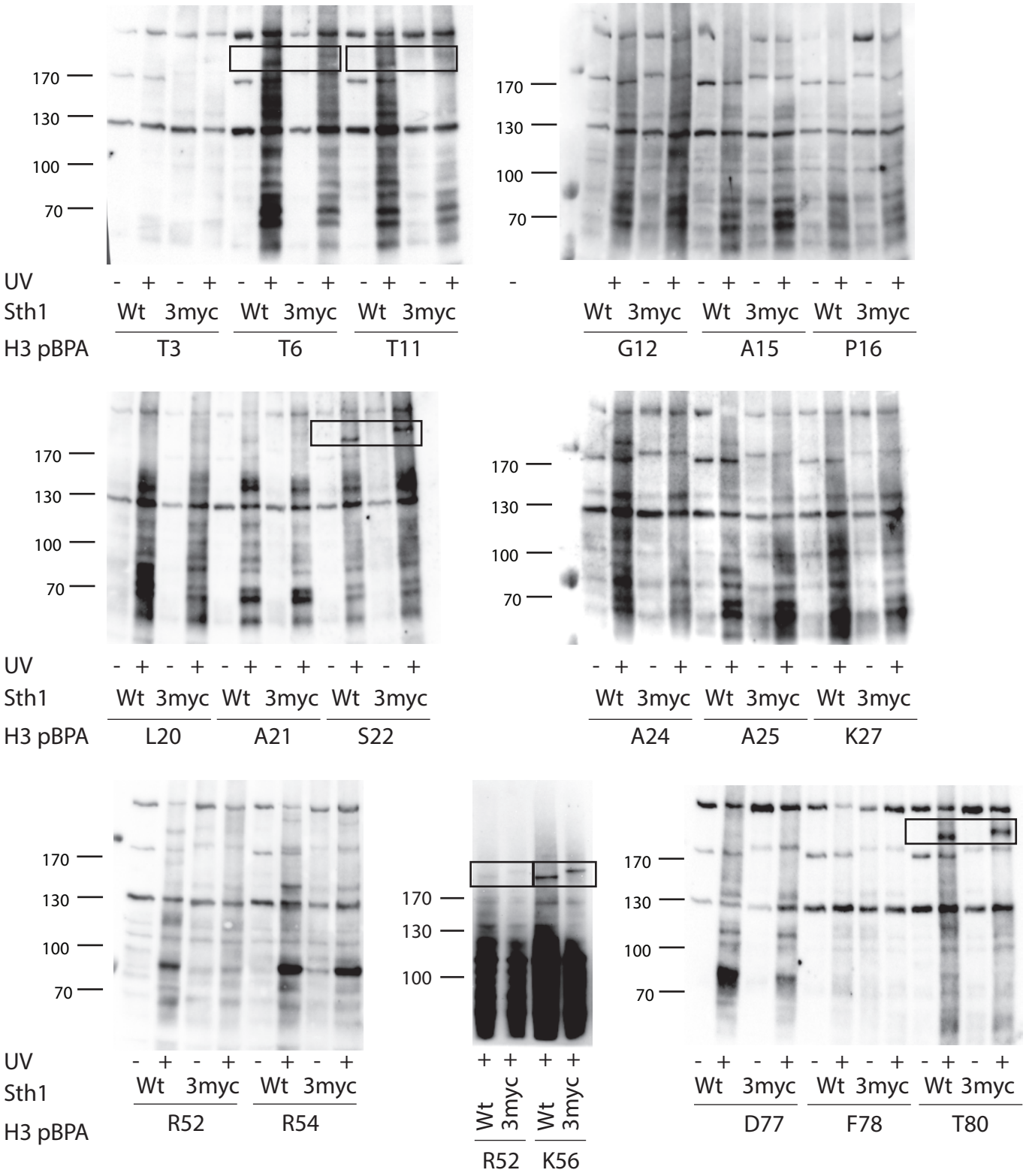

Supplemental Figure 5: Identification of Sth1-histone H3 crosslink products. Full-sized Western blots to Figure 1. Yeasts (wild-type or Sth1-3myc) expressing the indicated pBPA-containing histone were UV-irradiated and whole cell lysates analysed by SDS-PAGE and Western Blot using anti-HA antibodies. Boxed areas show bands sensitive to Sth1-tagging.

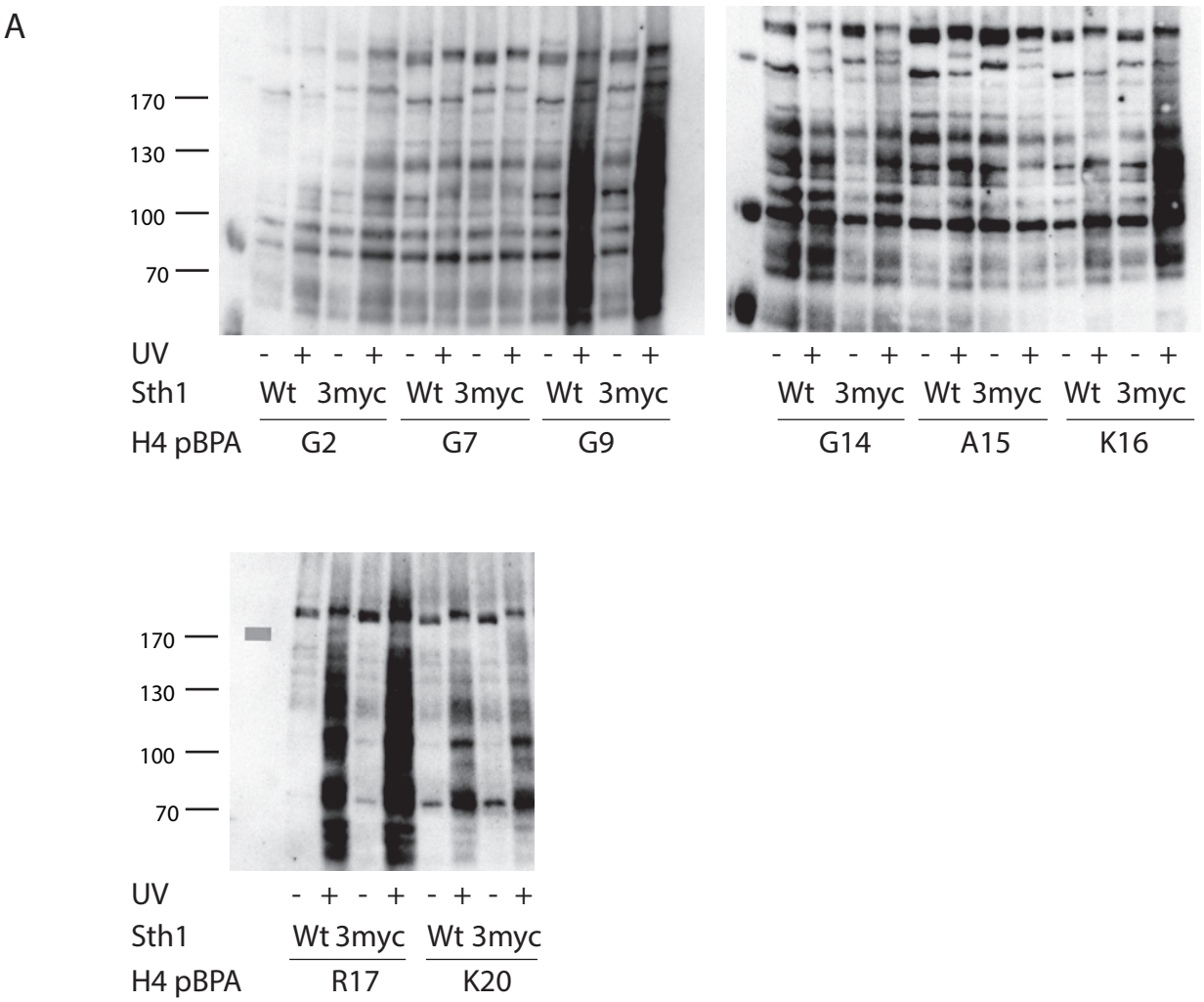

Supplemental Figure 6: A) Identification of Sth1-histone H4 crosslink products. Full-sized Western blots to Figure 1a. Yeasts (wild-type or Sth1-3myc) expressing the indicated pBPA-containing histone were UV-irradiated and whole cell lysates analysed by SDS-PAGE and Western Blot using anti-HA antibodies. No significant shifts were detected. B) Full-sized Western blot to Figure 1b. The Sth1-histone crosslink is indicated by the arrowhead. A cross-reactive band is marked by an asterisk. An independent replicate is shown on the right.

A

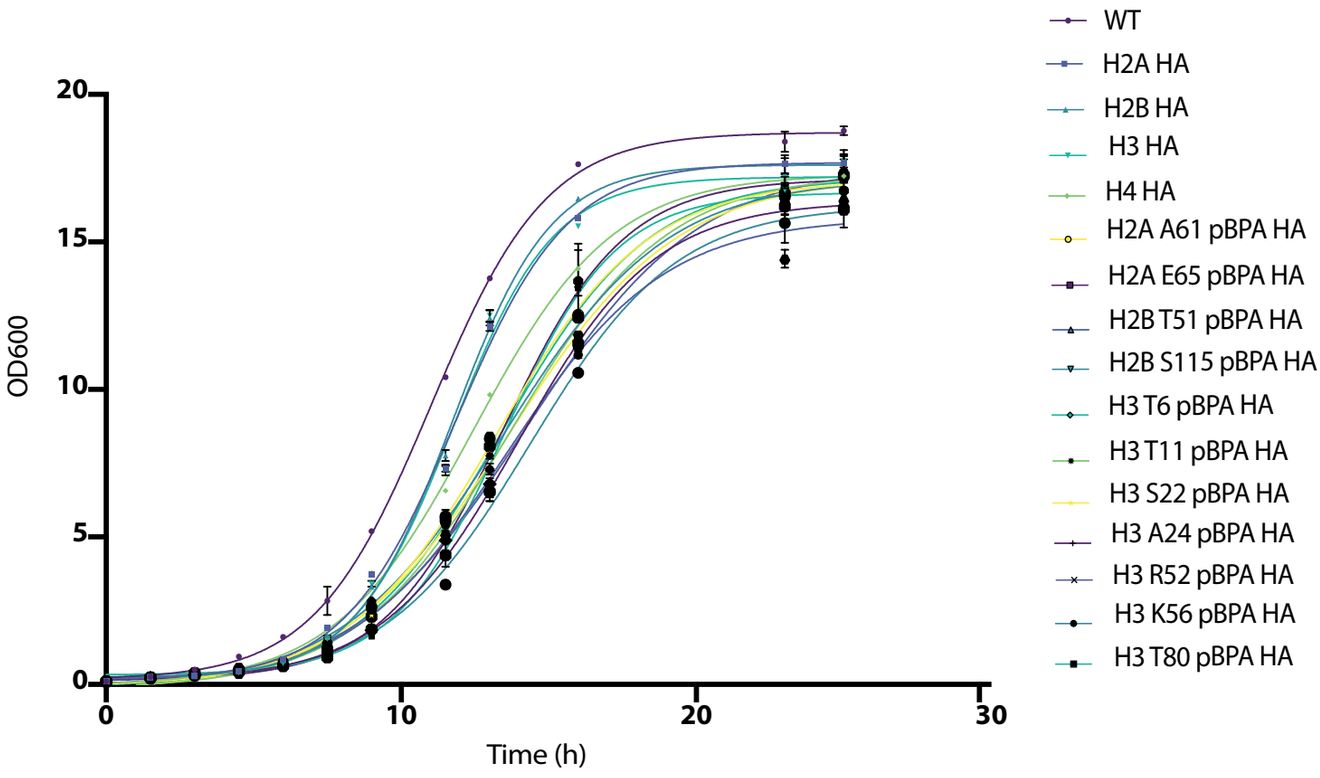

B

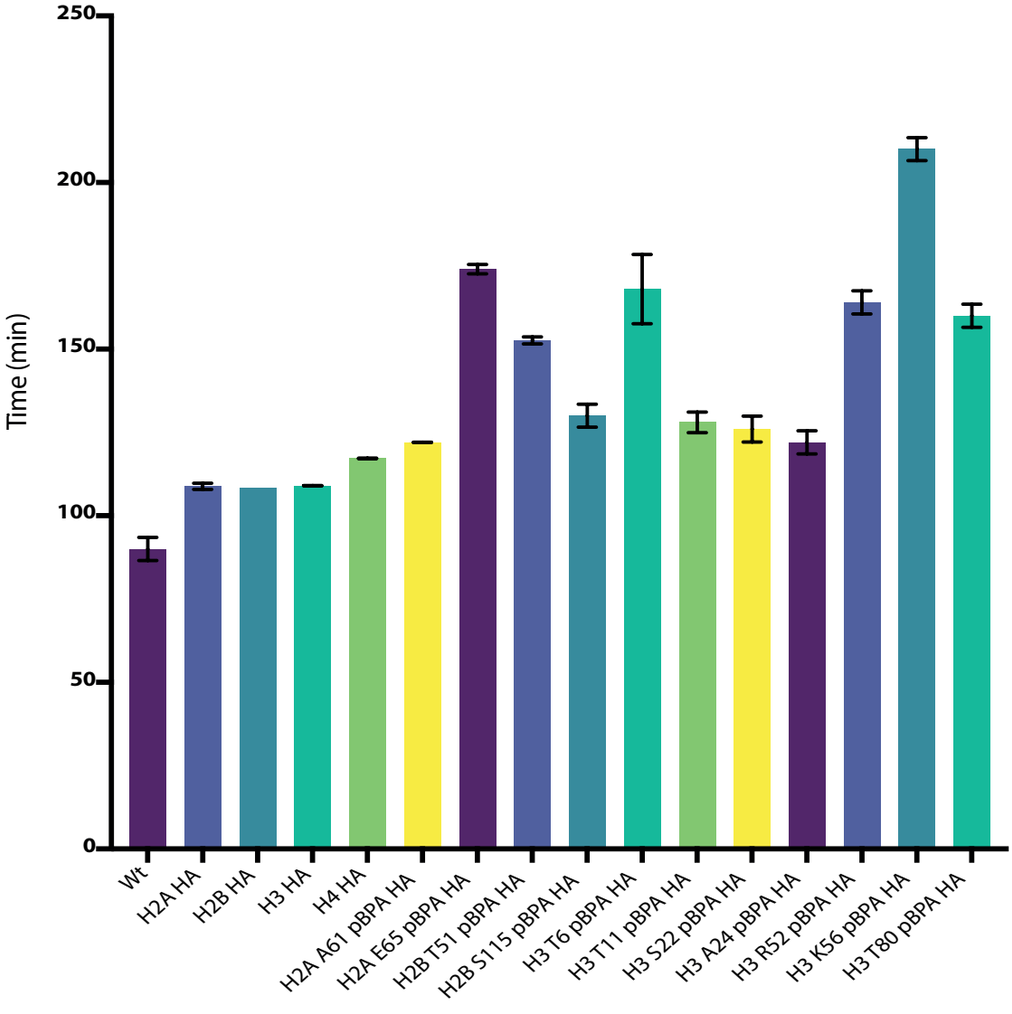

Supplemental Figure 7: Comparative growth of Wildtype and Histone pBPA-mutants. Related to Figure 1.

A. BY4741 cells were grown in YPD medium and BY4741 expressing the indicated Histone pBPA-mutants in the presence of the pBPARS/tRNA pair were grown in minimal medium (SD -Leu,-Ura). Overnight cultures were diluted to OD600 = 0.1 and growth was monitored at indicated time points for biological triplicates of all samples. Growth curves were plotted using Boltzmann sigmoidal curve fitting option in Graphpad Prism 8 Software. Data are represented as mean ± SD.

B. Doubling time of Wildtype and Histone pBPA-mutants was calculated using growth curve in (A). Data are represented as mean ± SD.

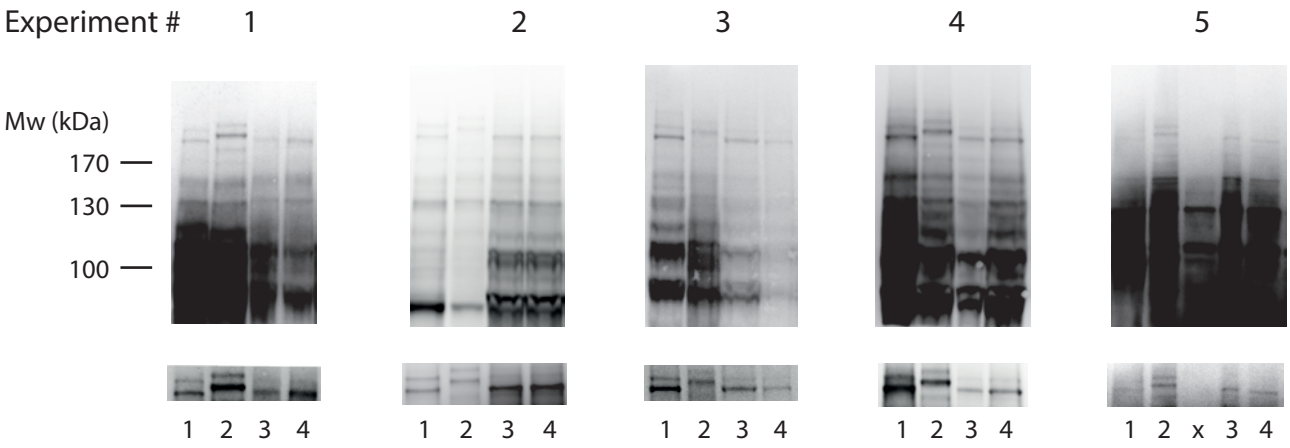

	1	2	3	4
H2B T51pBPA:	WT	WT	K6R, K7R, K16R, K17R	WT
Genotype:	WT	Sth1 3myc	WT	Δsiz1 Δsiz2

Supplemental Figure 8: Full sized Western blots to Fig. 3

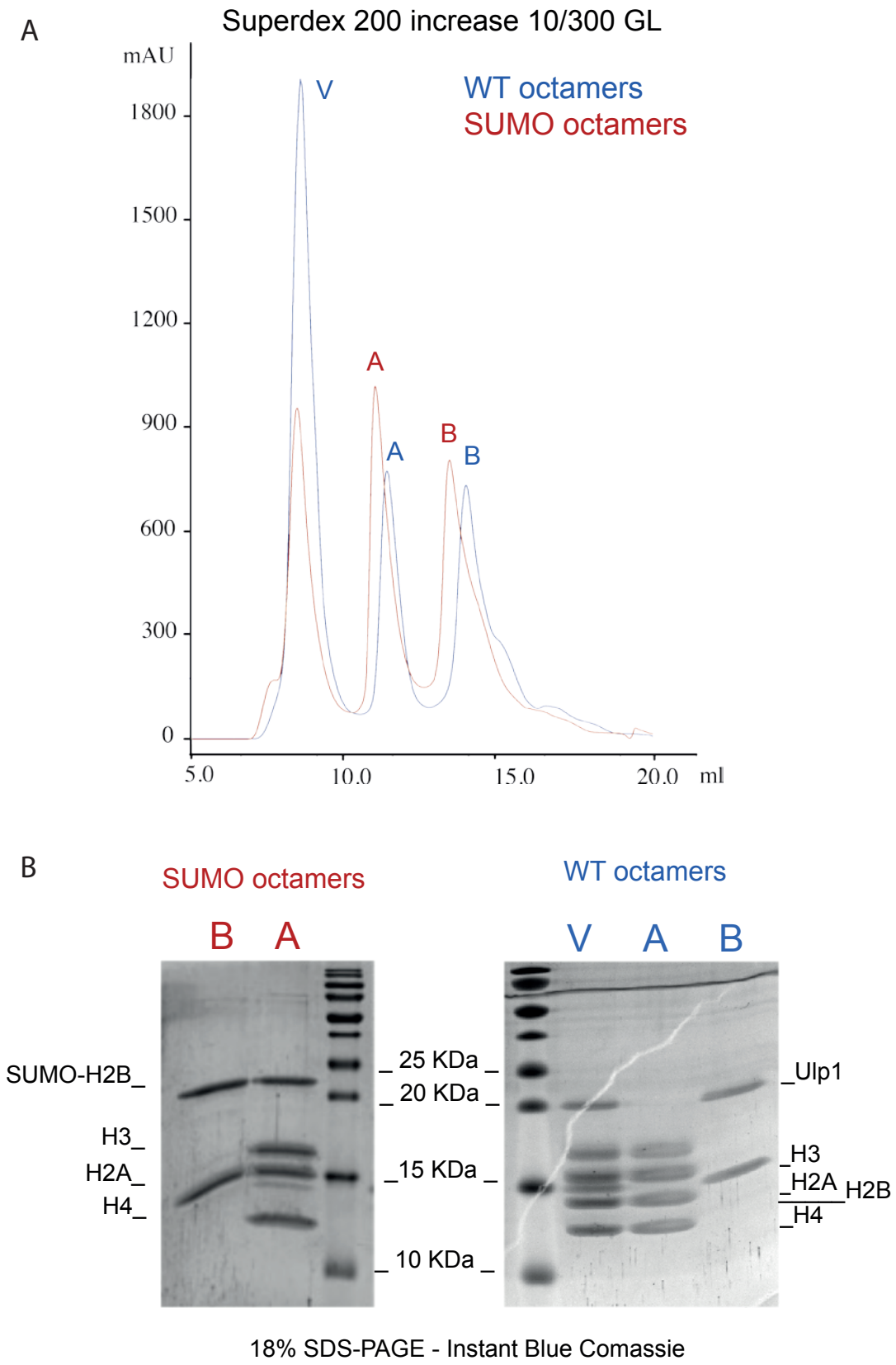

Supplemental Figure 9: SUMOylated octamers were expressed in E. coli and purified via Ni-NTA. Related to Figure 4. A) Elutions from Ni-NTA column were loaded in Superdex 200i GL 10/300 column. The first peak contained aggregates, peak A contained correctly refolded octamers while peak B showed the excess H2A/B dimers. B) SDS-PAGE analysis of histone octamers. To obtain WT octamers, SUMOylated octamers were digested with SUMO protease (Ulp1) and subjected to size exclusion chromatography again.

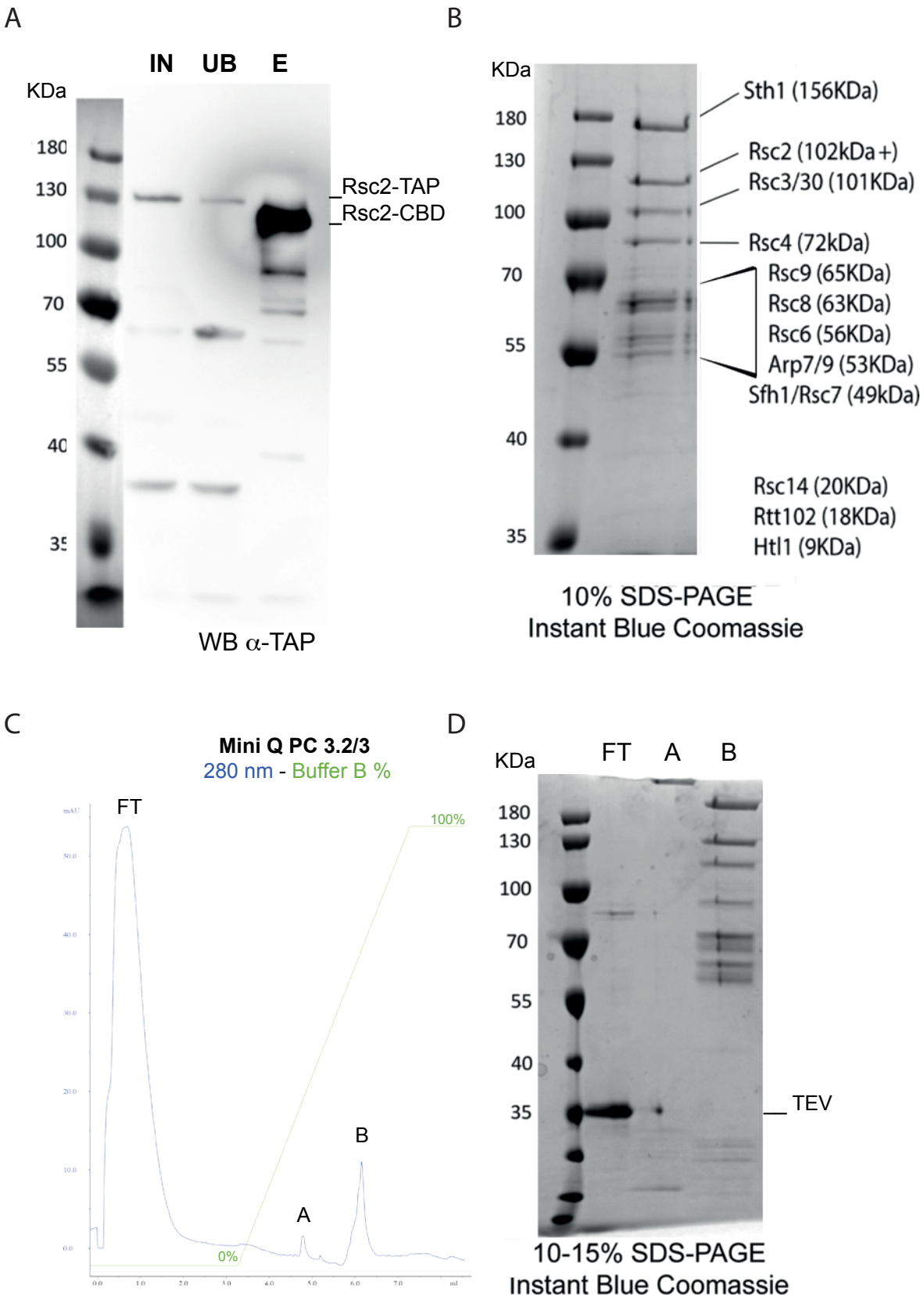

Supplemental Figure 10: RSC complex purified from yeast via Rsc2-TAP. Related to Figure 4. A) Western blotting of clarified lysate (IN) and flow-through after IgG-sepharose beads binding (FT), alongside with eluate after TEV-cleavage (E) analyzed on 4-12% SDS-PAGE and blotted for anti-TAP antibody. The two bands correspond to the RSC2-TAP before and after cleavage. B) After elution, the RSC complex was analyzed by 10% SDS-PAGE and stained with Instant Blue Coomassie. C) In order to perform measurements on the BLI, the RSC complex was biotinylated with tenfold molar excess of NHS-biotin. After quenching the reaction, the RSC was further purified via anion exchange in linear gradient from Buffer A to buffer B. D) RSC eluted at 650 mM KOAc as confirmed by SDS-PAGE.

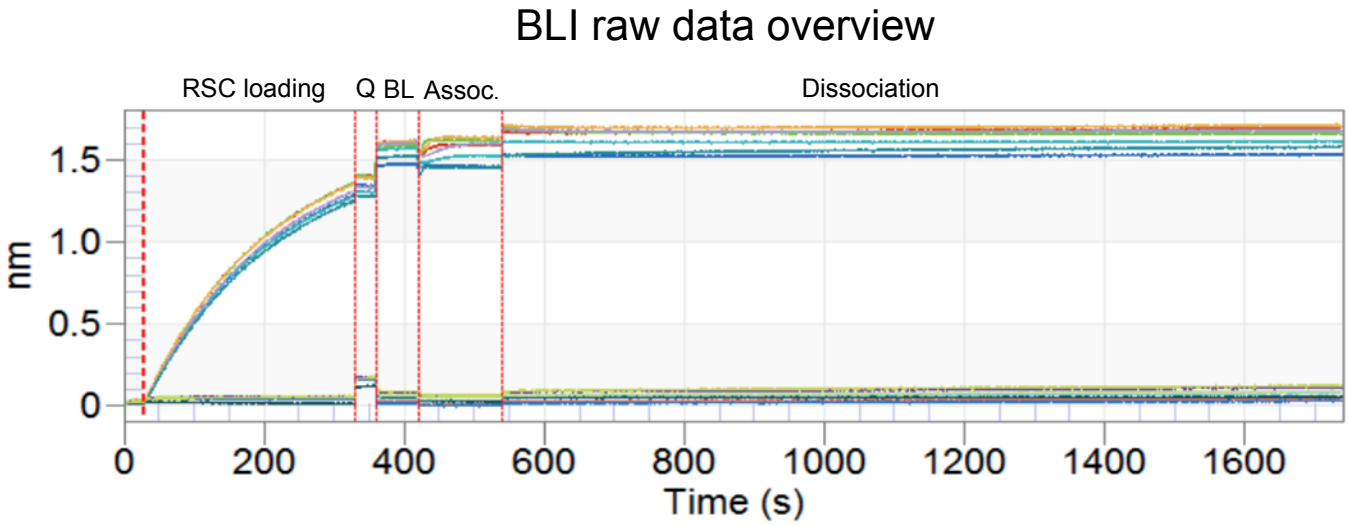

Supplemental Figure 11: BLI raw data graph, related to Fig. 4A&B.

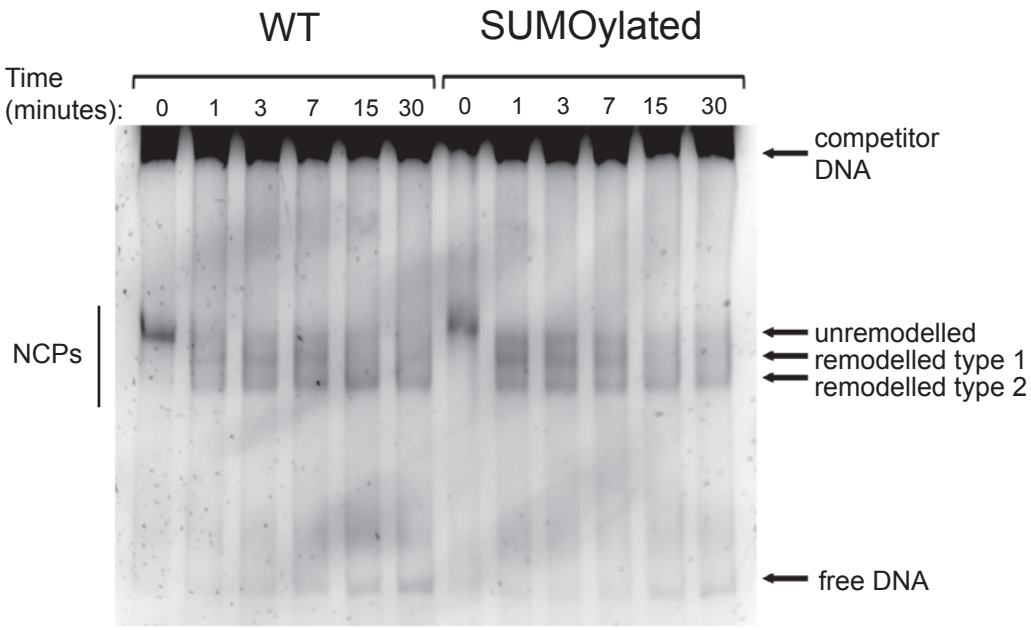

Supplemental Figure 12: RSC remodelling reactions were analysed by EMSA. Bands for nucleosomes, two remodelled species and free DNA were quantified densitometrically. Data from three independent experiments are plotted in Fig. 4E-G.

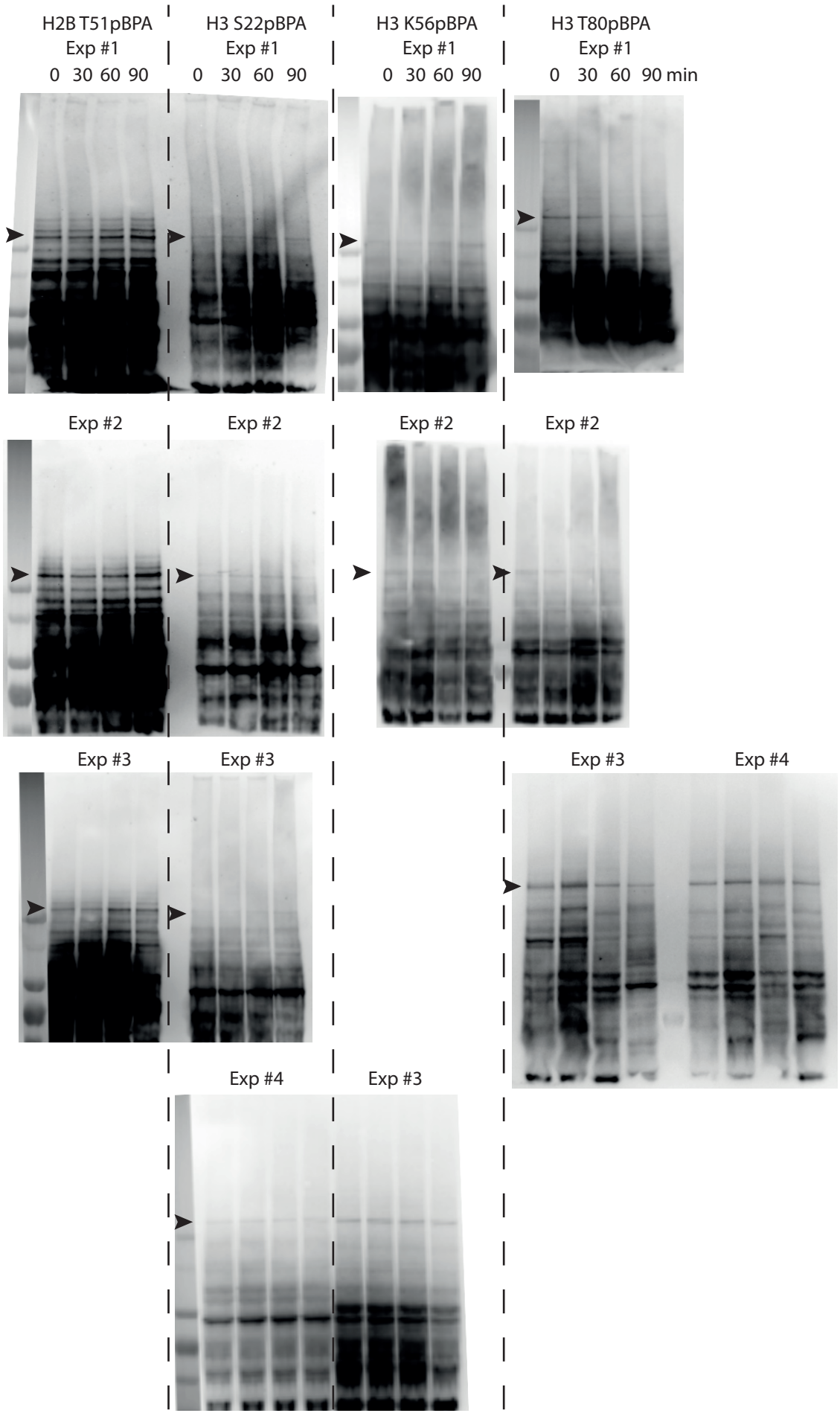

Supplemental Figure 13: Cell cycle dependence of Sth1-histone crosslinks.
Full sized Western blots to Fig. 5.

Supplemental Table S1. Yeast strains, related to *Transparent Methods.*

Strain	Genotype	Reference
BY4741	*Mat a his3Δ1 leu2Δ0 met15Δ0 ura3Δ0*	
BY4741 Sth1-3myc	[BY4741] *Sth1-3Myc::HIS3MX6*	This study
BY4741 Δ*gcn5*	[BY4741] *gcn5::HIS3*	This study
BY4741 Δ*siz1* Δ*siz2*	[BY4741] *siz1::kanMX siz2::hphNT1*	This study
BJ3505 Rsc2-TAP	*MATα pep4::HIS3 prb1-Δ1.6R lys2-208 trp1-Δ101 ura3-52 gal2 can1 rsc2-TAP::klTRP leu2Δ::KAN*	This study
W303a *cdc15-2*	*MATα leu2-3,112 trp1-1 can1-100 ura3-1 ade2-1 his3-11,15 phi+ cdc15-2*	(Spellman, et al., 1998)
S288C H3	*MATα his3Δ200 leu2Δ0 lys2Δ0 trp1Δ63 ura3Δ0 met15Δ0 can1::MFA1pr-HIS3 hht1-hhf1::NatMX4 hht2-hhf2::[HHTS-HHFS]*-URA3*	(Dai, et al., 2008)
S288C H3 K14A	*MATα his3Δ200 leu2Δ0 lys2Δ0 trp1Δ63 ura3Δ0 met15Δ0 can1::MFA1pr-HIS3 hht1-hhf1::NatMX4 hht2-hhf2::[HHTS K14A-HHFS]*-URA3*	(Dai, et al., 2008)

Transparent methods

Chemicals

Anti-HA antibody was obtained from Abcam (ab9110), pBPA from Chem-Impex. Other materials and media were used as reported previously (Hoffmann, et al., 2018).

Yeast strains and plasmids

Histone amber mutants were created by QuikChange mutagenesis on pRS426 plasmids encoding a C-terminally HA-tagged histone under the control of its native promoter and verified by sequencing the entire ORF (Hoffmann, et al., 2018). pCDF-ScNap1 was created by cloning the *NAP1* ORF in pCDF-DUET using restriction sites BamHI/SalI. pQE80-His_{14}-SUMO-H2B was created by cloning the *Xenopus* H2B-ORF lacking the first five codons in pQE80-His_{14}-SUMO (a kind gift of Dirk Görlich, Göttingen) using restriction sites KpnI/SpeI. Histone octamers containing SUMOylated H2B were produced using a plasmid encoding for all four human core histones in which the ORF of H2B was replaced by the ORF of pQE80-His_{14}-SUMO-H2B. Plasmids encoding multiple repeats of Widom-601 sequences were gifts of Fabrizio Martino and Daniela Rhodes.

Yeast strains used in this study are listed in Table S1. BY4741 Sth1-3myc was obtained by integrating three myc-epitopes followed by the *HIS3MX6* cassette of pYM5 (Knop, et al., 1999) prior to the translational stop codon of the *STH1* gene using standard PCR-based tagging. BJ3505-Rsc2-TAP was created in analogous fashion by integrating CBP-TEV-protA at the end of the RSC2 ORF using plasmid pBS1479 (Puig, et al., 2001). Successful integration was verified by PCR and Western blot.

BY4741 Δ*siz1* Δ*siz2* was created in two sequential rounds of genomic integrations. First, the *kanMX* box was used to replace the *SIZ1* locus in BY4741 by a PCR product amplified from pUG6 (Guldener, et al., 1996) with flanking sequences homologous to the *SIZ1* 5'- and 3'-UTR. Successful replacement was verified by PCR of geneticin resistant clones. Next, *SIZ2* was replaced by genomic integration of the *hphNT1* box amplified from pYM24 (Janke, et al., 2004) in the same manner using hygromycin B selection.

BY4741 Δ*gcn5* was established through genomic integration of the *HIS3* gene at the *GCN5* locus. Standard PCR amplification of the pRS303 plasmid was performed to amplify the *HIS3* region with flanking sequences homologous to the *GCN5* 5'- and 3'-UTR. Genomic integration was selected with SC-His dropout agar and surviving colonies were verified by PCR.

Photo-crosslinking of living yeast

Yeast photo-crosslinking experiments were carried out as described (Hoffmann, et al., 2018). Briefly, yeasts were transformed with plasmids to encode pBPA-containing histones and grown in SC-Ura/Leu with 1 mM pBPA. For crosslinking, 12 OD units were harvested, irradiated (365 nm) for 15 min on ice, proteins extracted by alkaline lysis and precipitated with TCA. Crosslinks were analysed by 3-8% Tris-acetate SDS-PAGE and Western blot.

Blots were developed by measuring chemiluminescence (ECL Select, GE Healthcare) with an imaging system (Celvin S, Biostep). Quantification of band intensities were performed with Fiji software on raw inverted tiff images of Western blots. Therefore, the image was rotated so that lanes ran horizontally. A box was drawn across an individual lane using the "rectangle" tool and grey density analysed by "Plot profile". The peak corresponding to the protein band was traced using the "free hand selection" tool and the peak area analysed using "measure". Normalization of the measured intensity was done to the background. Average mean intensity and standard deviations were calculated for three biological replicates.

Yeast cell cycle synchronization

Cell cycle synchronizations were performed in W303a cells with a temperature-sensitive *cdc15-2* allele containing plasmids encoding H2B or H3 pBPA-mutants (Hoffmann, et al., 2018). An overnight culture of 4 ml in SC-Ura/Leu minimal medium (supplemented with 1 mM pBPA) was diluted to an OD600 = 0.2 in 50 ml YPD and incubated with shaking at 25°C until an OD600 of 0.5 was reached. Cells were then shifted for 2 h to 37°C with shaking to arrest cells in telophase (Surana, et al., 1993). Following complete arrest (as determined by FACS analysis (Haase, 2004)), cells were released into 50 ml YPD at an OD600 = 0.5 at 25°C. Samples were taken at indicated time points, crosslinked and processed as described above.

RSC purification

RSC complex was purified by tagging the C-terminus of the Rsc2 subunit with a TAP tag in BJ3505 essentially as described (Fig. S10) (Puig, et al., 2001).

Nucleosome Reconstitution

Purification of Octamers: DNA-sequence from yeast *SMT3* was fused in frame to the K6 of *Xenopus* H2B in pQE80 incorporating an N-terminal His-tag. Because reconstitution of histone octamers from individually purified, recombinant histones by standard protocols was unsuccessful, we cloned SUMO-xH2B via Gibson Assembly into a pDUET plasmid for polycistronic coexpression (a gift from A. Musacchio) (Weir, et al., 2016). The final construct containing His_6H3.1-H4-His_6H2A1B-SUMO-H2B, was used to transform Rosetta2® *E. coli* cells. Expression and purification were carried out essentially as described (Shim, et al., 2012). After elution from the Ni-NTA column, the octamer-containing fractions were concentrated with an Amicon 10k. The His-tag was removed with 0.2 mg/ml GST-PreScission protease for 12 hours at 4°C. For the purification of deSUMOylated octamers, Ubl1 protease was added to the concentrated octamers to a final concentration of 0.2 mg/mL. The digested octamers were further

purified by gel-filtration (Superdex 200 10/300 GL, GE Healthcare) in 10 mM HEPES pH 7.4, 2.0 M NaCl, 0.5 mM EDTA, 1 mM TCEP (Fig. S9). Fractions containing the octamers were pooled and used for nucleosome reconstitution.

DNA purification: DNA for nucleosome reconstitution was obtained from a pUC18 plasmid containing 25 repeats of Widom 601 DNA with 25 bp overhang on both sides (a gift from D. Rhodes). The 197 bp array was digested out from the plasmid with AvaI and concentrated to 1 mg/mL. The plasmid backbone was precipitated by centrifugation at 14000 g for 30 minutes after 12 hours incubation at 4°C in 10 mM Tris pH 8, 700 mM NaCl, 10 mM $MgCl_2$, 1 mM EDTA, 6.5% PEG 8000. The DNA in the supernatant was precipitated with isopropanol and used for nucleosome reconstitution. For the nucleosomes employed in the BLI experiments, we used the 167 bp 601 Widom DNA, which was purified with a similar protocol but using EcoRV instead of AvaI.

Nucleosome Reconstitution: Increasing concentration of octamers were titrated against a fixed amount of 197 bp Widom DNA to accurately determine the best ratio of protein and DNA. To reconstitute the final nucleosomes, a dialysis bag containing 1 mL solution of 3.0 µM DNA and 3.0 µM octamers was inserted into a second dialysis bag containing 50 mL of 10 mM HEPES pH 7.4, 2.0 M NaCl, 0.5 mM EDTA, 1 mM TCEP, and the resulting double bag was dialysed at 4°C for 20 h against 5 L 10 mM HEPES pH 7.4, 35 mM KOAc, 0.5 mM EDTA, 5 mM 2-BME. The quality of the reconstitutions was assessed by 6% Native PAGE (Acrylamide/Bis-acrylamide 49:1 ratio) stained with Gel Red®.

Purification of scNap1
His-tagged scNap1 was expressed and purified in Rosetta2® *E. coli* cells essentially as described (Wittmeyer, et al., 2004). After Ni-NTA elution, Nap1 containing fractions were concentrated to 2 mg/mL and loaded on a Superdex 200 10/300 GL gel-filtration column (GE Healthcare) pre-equilibrated with 25 mM HEPES pH 7.4, 10% glycerol, 300 mM KCl, 2 mM $MgCl_2$, 1 mM DTT. 6xHis-scNap1 containing fractions were pooled, concentrated to 24 µM and stored at –80°C.

Nucleosome Remodelling Assay
All remodelling reactions were performed at 30°C in 15 µl volumes containing 10 nM RSC complex, 60 nM nucleosomes (197bp Widom-601 DNA), and 1.5 µM scNap1 in reaction buffer (10 mM HEPES pH 7.4, 250 mM KOAc, 2 mM $MgCl_2$, 0.6 mM ATP, 100 µg/mL BSA). Reactions were quenched with 600 ng lambda DNA and glycerol (5% final concentration) after 1, 3, 7, 15, or 30 minutes and kept at 30°C for additional 15 min after quenching before being shifted to 4°C. To address the high velocity of the reaction, the time 0 reactions were incubated for 1 minute with 0.6 mM ADP instead of ATP and quenched as previously described.

To assess nucleosome remodelling, 6 µl of remodelling reactions were loaded onto 6% Native PAGE gel (Acrylamide/Bis-acrylamide 49:1 ratio) in 0.4x TBE, run in 0.4x TBE buffer at 4°C for 90 min at 150 V, and stained with Gel Red®. Band intensities were analysed and quantified with ImageJ.

RSC-nucleosome binding kinetic
Binding kinetics of nucleosomes to the RSC were analyzed with an Octet 384. The RSC complex eluted from IgG-sepharose beads was biotinylated with 10-fold molar

excess of NHS-biotin at room temperature for 90 min. The reaction was then quenched with 25 mM Tris pH 8 for 10 min. The biotinylated RSC was further purified via strong anion exchange column (Mini Q) pre-equilibrated with Buffer A (5% glycerol, 10 mM HEPES pH 8.0, 200 mM KOAc, 0.5 mM EDTA, 0.5 mM TCEP) and eluted with a linear gradient up to 100% Buffer B (5% glycerol, 10 mM HEPES pH 8.0, 1 M KOAc, 0.5 mM EDTA, 0.5 mM TCEP). RSC typically eluted at 700 mM KOAc. Immediately after elution, the complex was loaded onto Streptavidin (SA) biosensors. Successful loading of the RSC on the biosensor was confirmed by the shift in the interference patterns above 1.2 nm for all sensors (Fig. S11). After loading, the free binding sites on the sensors were quenched with 5 nM biotin. Buffers in baseline, association, and dissociation wells were 5% glycerol, 10 mM HEPES pH 8.0, 80 mM KOAc, 0.5 mM EDTA, 2.5 mM $MgCl_2$, 0.5 mM AMP-PNP, and 0.3 mg/mL BSA. In addition, association wells contained either WT or SUMOylated 601-167bp nucleosome at 22, 66, or 200 nM. For the binding kinetics analysis, raw data were analyzed with ForteBio Data Analysis 9.0. Briefly, all signals were processed with subtraction of the reference wells, aligned in the Y axis and in the inter-step correlation to the association, Savitzky-Golay filter was applied. The read-outs of each binding event were then plotted on GraphPad to determine the amplitude and to calculate the K_D.

RSC ATPase Activity

To determine the Michaelis-Menten constant of RSC complex on both unmodified and SUMOylated nucleosomes reconstituted with the 197 bp 601 Widom DNA, we evaluated the ATPase activity of Sth1 with an ADP-Glo™Assay (Promega). The reactions were performed at 30°C in 30 µl containing 5% glycerol, 10 mM HEPES pH 7.4, 120 mM KOAc, 150 µg/mL BSA, 2.5 mM $MgCl_2$, 0.5 mM ultrapure ATP, 0.5 mM TCEP, and 10 nM RSC. After 5, 10, and 15 minutes 5 µl were quenched with ADP-Glo™ Reagent and analyzed as recommended by the supplier. All measurements were performed in triplicate and analyzed with GraphPad.

Supplemental References

Dai, J., Hyland, E.M., Yuan, D.S., Huang, H., Bader, J.S., and Boeke, J.D. (2008). Probing nucleosome function: a highly versatile library of synthetic histone H3 and H4 mutants. Cell 134, 1066-1078.

Guldener, U., Heck, S., Fielder, T., Beinhauer, J., and Hegemann, J.H. (1996). A new efficient gene disruption cassette for repeated use in budding yeast. Nucleic Acids Res 24, 2519-2524.

Haase, S.B. (2004). Cell cycle analysis of budding yeast using SYTOX Green. Curr Protoc Cytom Chapter 7, Unit 7 23.

Hoffmann, C., Neumann, H., and Neumann-Staubitz, P. (2018). Trapping Chromatin Interacting Proteins with Genetically Encoded, UV-Activatable Crosslinkers In Vivo. Methods Mol Biol 1728, 247-262.

Janke, C., Magiera, M.M., Rathfelder, N., Taxis, C., Reber, S., Maekawa, H., Moreno-Borchart, A., Doenges, G., Schwob, E., Schiebel, E., et al. (2004). A versatile toolbox for PCR-based tagging of yeast genes: new fluorescent proteins, more markers and promoter substitution cassettes. Yeast 21, 947-962.

Knop, M., Siegers, K., Pereira, G., Zachariae, W., Winsor, B., Nasmyth, K., and Schiebel, E. (1999). Epitope tagging of yeast genes using a PCR-based strategy: more tags and improved practical routines. Yeast 15, 963-972.

Puig, O., Caspary, F., Rigaut, G., Rutz, B., Bouveret, E., Bragado-Nilsson, E., Wilm, M., and Seraphin, B. (2001). The tandem affinity purification (TAP) method: A general procedure of protein complex purification. Methods 24, 218-229.
Shim, Y., Duan, M.R., Chen, X.J., Smerdon, M.J., and Min, J.H. (2012). Polycistronic coexpression and nondenaturing purification of histone octamers. Anal Biochem 427, 190-192.
Spellman, P.T., Sherlock, G., Zhang, M.Q., Iyer, V.R., Anders, K., Eisen, M.B., Brown, P.O., Botstein, D., and Futcher, B. (1998). Comprehensive identification of cell cycle-regulated genes of the yeast Saccharomyces cerevisiae by microarray hybridization. Mol Biol Cell 9, 3273-3297.
Surana, U., Amon, A., Dowzer, C., McGrew, J., Byers, B., and Nasmyth, K. (1993). Destruction of the CDC28/CLB mitotic kinase is not required for the metaphase to anaphase transition in budding yeast. EMBO J 12, 1969-1978.
Weir, J.R., Faesen, A.C., Klare, K., Petrovic, A., Basilico, F., Fischbock, J., Pentakota, S., Keller, J., Pesenti, M.E., Pan, D.Q., et al. (2016). Insights from biochemical reconstitution into the architecture of human kinetochores. Nature 537, 249-+.
Wittmeyer, J., Saha, A., and Cairns, B. (2004). DNA translocation and nucleosome remodeling assays by the RSC chromatin remodeling complex. Method Enzymol 377, 322-343.